Journal of Medicinal Chemistry

Article

pubs.acs.org/jmc

The Oncolytic Efficacy and in Vivo Pharmacokinetics of [2-(4-Chlorophenyl)quinolin-4-yl](piperidine-2-yl)methanol (Vacquinol-1) Are Governed by Distinct Stereochemical Features

Lars G. J. Hammarström,[*,†,#] Robert K. Harmel,[†,▽] Mikael Granath,[‡] Rune Ringom,[‡] Ylva Gravenfors,[§] Katarina Färnegårdh,[§] Per H. Svensson,[∥] David Wennman,[∥] Göran Lundin,[∥] Ylva Roddis,[∥] Satish S. Kitambi,[⊥] Alexandra Bernlind,[∥] Fredrik Lehmann,[‡] and Patrik Ernfors[⊥]

[†]Chemical Biology Consortium Sweden, Science for Life Laboratory, Division of Translational Medicine and Chemical Biology, Department of Medical Biochemistry and Biophysics and [⊥]Division of Molecular Neurobiology, Department of Medical Biochemistry and Biophysics, Karolinska Institutet, SE-171 77 Stockholm, Sweden

[‡]OnTargetChemistry AB, Virdings Allé 18, SE-754 50 Uppsala, Sweden

[§]Drug Discovery and Development Platform, Science for Life Laboratory, Department of Organic Chemistry, Stockholm University, Box 1030, SE-171 21 Solna, Sweden

[∥]SP Process Development, Forskargatan 20J, SE-151 36 Södertälje, Sweden

[#]Glionova Therapeutics, Västra Trädgårdsgatan 15, SE-111 53 Stockholm, Sweden

Supporting Information

ABSTRACT: Glioblastoma remains an incurable brain cancer. Drugs developed in the past 20 years have not improved the prognosis for patients, necessitating the development of new treatments. We have previously reported the therapeutic potential of the quinoline methanol Vacquinol-1 (**1**) that targets glioblastoma cells and induces cell death by catastrophic vacuolization. Compound **1** is a mixture of four stereoisomers due to the two adjacent stereogenic centers in the molecule, complicating further development in the preclinical setting. This work describes the isolation and characterization of the individual isomers of **1** and shows that these display stereospecific pharmacokinetic and pharmacodynamic features. In addition, we present a stereoselective synthesis of the active isomers, providing a basis for further development of this compound series into a novel experimental therapeutic for glioblastoma.

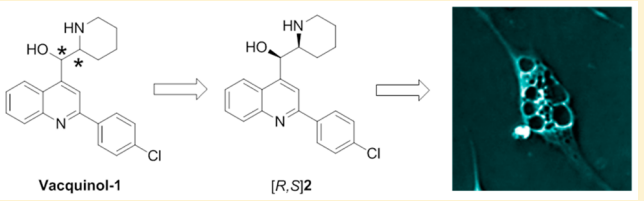

INTRODUCTION

Despite decades of efforts to develop improved therapies, glioblastoma (GBM, WHO grade IV astrocytoma) remains the most common and lethal of all primary brain tumors.[1,2] Even with the aggressive current standard therapy comprising surgical resection, followed by radiation and Temozolomide (TMZ) chemotherapy, median overall survival for GBM patients is a mere 12−14 months.[3] GBM is characterized by an infiltrative dissemination of cancer-initiating cells from the primary tumor into surrounding brain parenchyma, attenuating the efficacy of surgical resection. Nearly 100% of patients recur with secondary tumors that are highly refractive to chemotherapy and radiation.[4,5] The FDA-accelerated approval of the monoclonal anti-VEGF-A antibody bevacizumab as first line therapy for recurrent GBM in the United States offered hope for better treatment; however, recent clinical results of this antiangiogenic therapy suggest no significant benefit on overall survival.[1,6−9]

The difficulties of developing efficacious GBM therapies are exacerbated by the central nervous system (CNS) location of the tumor, requiring penetration of the blood−brain barrier (BBB),[10−12] and marked mutational heterogeneity of this cancer.[13−15] Due partially to the complexity of GBM genetics, targeted therapy approaches have largely failed in the clinical setting, requiring the discovery of new approaches to tackle the disease.[16]

We have previously described a series of quinoline methanols, named Vacquinols, which act as oncolytic agents and target patient-derived GBM cells by a mechanism of action not previously explored therapeutically.[17] These compounds[18−20] stem from an effort to develop more efficient antimalarial compounds during the 1940s−60s, as chloroquine-resistant *Plasmodium falciparum* increased in incidence.[21,22] Vacquinols selectively induce catastrophic vacuolization in GBM cells at low micromolar concentrations and, within hours, result in apoptosis-independent lysis. Although the precise molecular mechanisms of action are yet to be resolved, Vacquinols appear to act independently of the genetic profile of GBM and are efficacious in vitro on all subclasses of GBM.[17]

Received: July 9, 2016
Published: September 8, 2016

DOI: 10.1021/acs.jmedchem.6b01009
J. Med. Chem. 2016, 59, 8577−8592

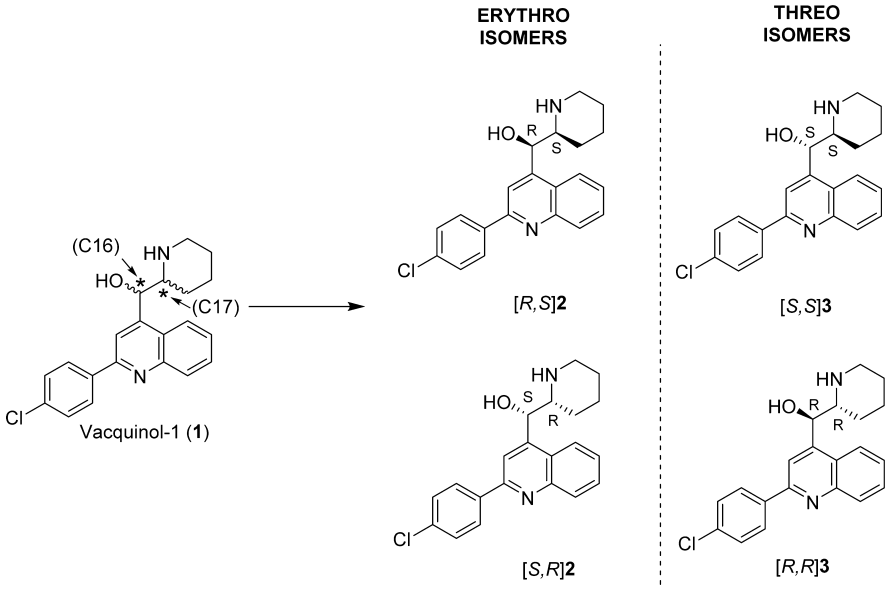

Figure 1. Structure of **1**, stereogenic centers at C16 (α to quinoline) and C17 (β to quinoline) denoted with an asterisk (*) and the corresponding *erythro* ([*R*,*S*]**2** and [*S*,*R*]**2**), and *threo* ([*S*,*S*]**3** and [*R*,*R*]**3**) isomers, respectively.

An early lead compound in this series, (2-(4-chlorophenyl)-quinolin-4-yl) (piperidin-2-yl)methanol (NSC13316, **1**) is orally bioavailable, readily penetrates the BBB, and has favorable preclinical characteristics.[17]

Compound **1** is a mixture of four stereoisomers, namely the *erythro* (syn) isomers [*R*,*S*]**2** and [*S*,*R*]**2**, and *threo* (anti) isomers [*S*,*S*]**3** and [*R*,*R*]**3**, resulting from the two adjacent stereogenic centers at C16 and C17 (Figure 1). As each of these isomers potentially exhibit differential metabolism, pharmacokinetics and pharmacology, the further development of **1** as an isomeric mixture into an investigational drug for the treatment of glioblastoma is challenging (the use of the nomenclature "Vacquinol-1", or compound **1**, in this manuscript will hereafter refer to the mixture of all four isomers).

Here, we describe the isolation and characterization of the individual isomers of **1** and show that stereochemistry dictates not only in vitro efficacy but also tissue exposure profiles and pharmacokinetics. We show that the *erythro* isomer (*R*)-[2-(4-chlorophenyl)quinolin-4-yl](2*S*)-piperidin-2-ylmethanol ([*R*,*S*]**2**) is superior to the other isomers in terms of efficacy and brain tissue exposure. In addition, we present efficient methods to access the individual isomers of **1** and related analogs through stereoselective synthesis.

RESULTS AND DISCUSSION

Chromatographic Isolation of the Isomers of 1. Compound **1** was prepared as previously described,[17] and the stereoisomers isolated chromatographically using both standard and chiral columns. Preparative HPLC of 300 mg **1** using a standard-phase Kromasil silica column efficiently separated the *erythro* from the *threo* racemates, eluting in approximately equal quantities into fractions denoted *I* and *II* without stereochemical assignment. Fraction *I* was next separated using semipreparative HPLC using a Chiralcel OD-H column into enantiomerically pure fractions *Ia* and *Ib*, in similar quantities. Fraction *II* was successfully separated using a Chiralpak AD-H column, resulting in fractions *IIa* and *IIb* (Figure 2). The individual isomers were obtained with acceptable recovery, high purity, and high enantiomeric excess as assessed by polarimetry and analytical HPLC using chiral columns (Figure S1). The results show that **1** is a mixture of four stereoisomers in approximately equal quantities and that these can be efficiently isolated and purified for individual characterization using chromatographic techniques employing chiral columns.

Comparative in Vitro Evaluation of 1 Isomers on Patient-Derived Human Glioblastoma Cells Reveals Stereospecific Pharmacodynamics. After isolation of the stereoisomers of **1**, we next compared their relative in vitro oncolytic efficacy in an ATP-based in vitro viability assay. Human patient-derived U3013 glioblastoma cells (3000 cells/well) were dispensed and allowed to adhere and proliferate for 24 h in a black, clear-bottom 384-well plate (PerkinElmer) as previously described.[17] Fractions *Ia*, *Ib*, *IIa*, and *IIb* (corresponding to each stereoisomer of **1**) were serial diluted into quadruplicate wells to 9 final concentrations ranging from 50 μM to 10 nM, and the plate was incubated for 48 h. DMSO (0.5%) and staurosporine (1 μM) were used as negative and positive controls, respectively. The cells were monitored using light microscopy at 4 h intervals for the appearance of the vacuolization phenotype at each concentration. After 48 h, viability of the cells in each well was evaluated by visual inspection and ATP quantification (CellTiterGlo, Promega) and compared to control.

The data showed a modest but robust superiority of fractions *IIa* and *IIb*, with an average IC_{50} of 3.5 and 3.8 μM, respectively; in comparison to fractions *Ia* and *Ib*, which exhibited IC_{50} values of 9.9 and 10.5 μM, after 48 h (Figure 3A). In addition, microscopic inspection of the cells at 5 μM concentrations of *IIa* between 4 and 8 h confirmed massive vacuolization as the mechanism of cell death, characteristic of this compound series (Figure 3B).[17] Vacuolization was markedly reduced in the presence of fractions *Ia* and *Ib* (data not shown). The cellular phenotype induced by fraction *IIa* was consistent with the previously described effects of **1**, i.e., catastrophic vacuolization as a result of macropinocytosis.[17] This phenotype is reminiscent of the cellular process described as methuosis, which is characterized by a displacement of the cytoplasm by large vacuoles of varying sizes resulting in loss of

DOI: 10.1021/acs.jmedchem.6b01009
J. Med. Chem. 2016, 59, 8577−8592

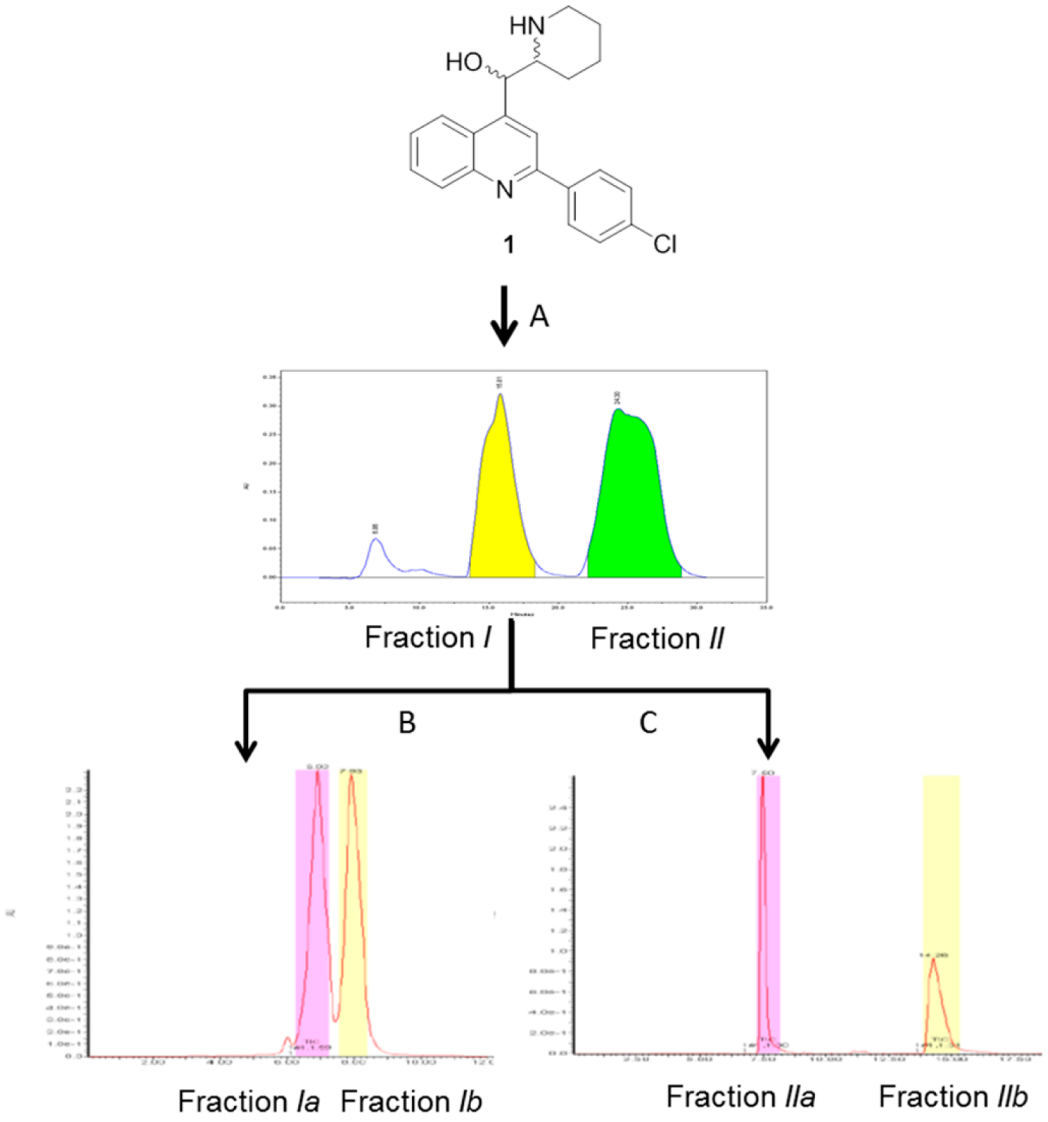

Figure 2. (A) Preparative HPLC-UV (265 nm) chromatographic separation of the *threo* and *erythro* isomers of **1** resulting in fractions *I* (yellow peak, t_R = 15.81 min) and *II* (green peak, t_R = 24.30 min). Kromasil silica (100 A) 10 μm, 50 × 190 mm column at an ambient temperature. Eluent: ethanol and *n*-heptane (1:1) with 0.2% diethyl amine additive in both phases. Flow rate: 100 mL/min. (B) Semipreparative HPLC-UV (265 nm) chromatographic separation of fraction *I* resolved into fractions *Ia* (pink peak, t_R = 6.9 min) and *Ib* (yellow peak, t_R = 7.9 min) using a chiral column. Chiralcel OD-H μm 20 × 250 mm column held at 22 °C. Eluent: ethanol/*n*-heptane (1:9) with 0.2% diethyl amine additive to both phases. Flow rate: 20 mL/min. (C) Semipreparative HPLC-UV (265 nm) chromatographic separation of fraction *II* resolved into fractions *IIa* (pink peak, t_R = 7.5 min) and *IIb* (yellow peak, t_R = 14.3 min). Chiralpak AD-H column 5 μm 20 × 250 mm column held at 35 °C. Eluent: ethanol/*n*-heptane (3:7) with a 0.2% diethyl amine additive to both phases. Flow rate: 20 mL/min.

plasma membrane integrity and necrosis-like cell death.[23−27] In summary, these data suggest that the primary in vitro phenotypic and oncolytic effects of **1** are driven primarily by fractions *IIa* and *IIb*, later confirmed to be *erythro* isomers [*R*,*S*]**2** and [*S*,*R*]**2** (see next section).

Crystallization and Absolute Stereochemical Assignment of the *erythro* Isomers of 1. Motivated by the in vitro activity of fractions *IIa* and *IIb*, we next assigned the absolute stereoconfiguration to these fractions using single crystal X-ray diffraction (SXRD). The isolated materials in fractions *IIa* and *IIb* were crystalline but contained only one-dimensional crystals, thus requiring optimization of crystallization procedures. Predictions using SIT software[28] indicated that chloroform would have high affinity for the crystal lattice. Crystallization of both fractions in chloroform, using both free-interface diffusion and solvent evaporation, provided crystals suitable for SXRD. The determined crystal structures (Figure 4) were chloroform solvates (compound:$CHCl_3$, 1:2), with one of the chloroform molecules disordered. Flack's X chirality parameters were used to determine absolute configuration.[29] In accordance with the calculated Flack parameter and the Cahn−Ingold−Prelog sequence rules,[30] the stereochemistry of carbons C16 and C17 (as indicated in Figure 1) was determined. Fraction *IIa* was determined to be *erythro* stereoisomer (*R*)-[2-(4-chlorophenyl)quinolin-4-yl]-(2*S*)-piperidin-2-ylmethanol ([*R*,*S*]**2**) and *IIb* was assigned as *erythro* stereoisomer (*S*)-[2-(4-chlorophenyl)quinolin-4-yl]-(2*R*)-piperidin-2-ylmethanol ([*S*,*R*]**2**), thus we could infer that fractions *I* and *II* were composed of the *threo* and *erythro* isomers, respectively. Polarimetry confirmed the enantiomeric relationship of these stereoisomers. Specific optical rotation of [*R*,*S*]**2** was determined to be +14.1° and its enantiomer [*S*,*R*]**2**

DOI: 10.1021/acs.jmedchem.6b01009
J. Med. Chem. 2016, 59, 8577−8592

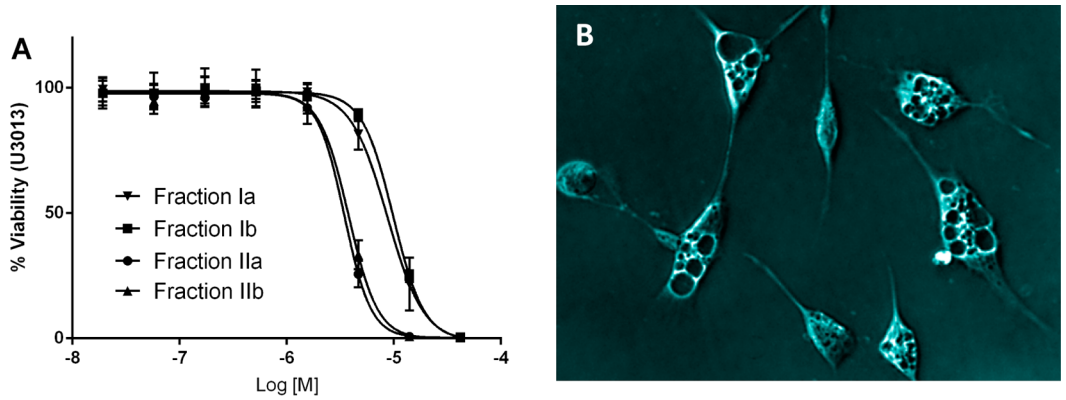

Figure 3. (A) Dose−response evaluation of isolated fractions from chromatographic separation of the isomers of **1** after 48 h incubation on U3013 glioblastoma cells showing a modest but robust superiority of fractions *IIa* (3.79 ± 0.28 μM) and *IIb* (3.46 ± 0.35 μM) (later assigned as *erythro* isomers [*R*,*S*]**2** and [*S*,*R*]**2**, respectively) versus fractions *Ia* (9.91 ± 0.92 μM) and *Ib* (10.5 ± 1.28 μM), representing *threo* isomers [*R*,*R*]**3** and [*S*,*S*]**3**. Data are presented as mean values of quadruplicate experiments with standard error. (B) Imaging of incubated U3013 cells in the presence of fraction *IIa* ([*R*,*S*]**2**) at 5 μM concentration for 4 h indicates accumulation of large, lucent intracellular vacuoles prior to cell death; thus verifying catastrophic vacuolization through hyper-stimulation of micropinocytosis as the mechanism of cytotoxicity. (The image is presented in negative exposure mode. Color and contrast have been adjusted for clarity.)

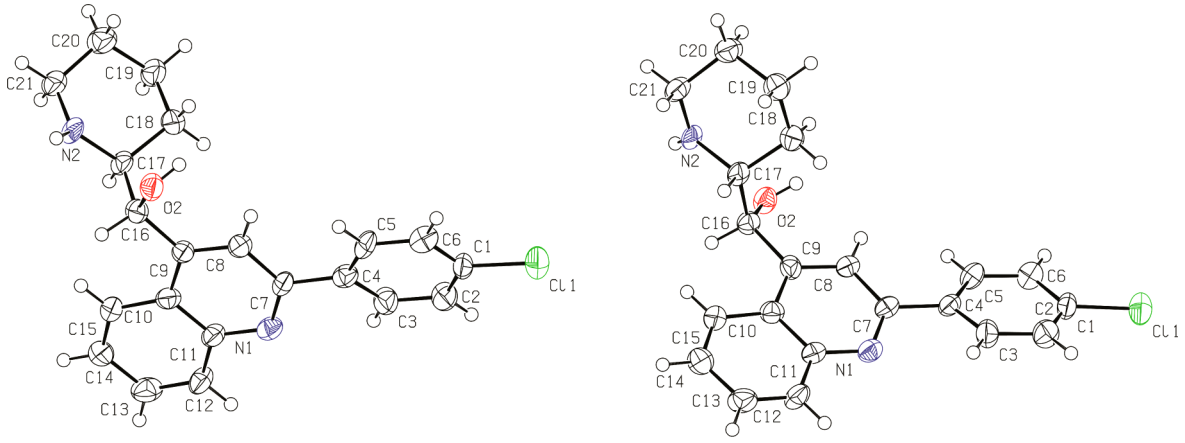

Figure 4. Molecular structures (Ortep) showing the absolute stereoconfiguration of *erythro* fractions *IIa* (left, [*R*,*S*]**2**) and *IIb* (right, [*S*,*R*]**2**). The molecular structures are obtained from the determined crystal structures.

was −14.3° when measured in chloroform at 25 °C. Polarimetry of compounds [*R*,*R*]**3** and [*S*,*S*]**3** resulted in +19.3 and −18.9 under the same conditions (Figure S1).

The stereochemical assignment of these fractions and characterization of their HPLC retention times, optical rotation, and the characteristic ^{1}H NMR spectra of the *erythro* and *threo* analogs (Figure 5) allowed for an efficient method to assign absolute and/or relative configuration of obtained compounds in the syntheses described below. For further information regarding crystal structure determination and optical rotation, see the Experimental Section. Complete ^{1}H and ^{13}C NMR spectra for the individual fractions obtained from chromatographic purification, confirmed to correspond to [*R*,*R*]**3**, [*S*,*S*]**3**, [*R*,*S*]**2** and [*S*,*R*]**2**, are available as Figures S2−S5.

Nonstereoselective Syntheses and in Vitro Efficacy of Novel Vacquinol Analogs. Earlier described syntheses of **1** and related compounds from this class have allowed only for preparation of the compound as a mixture of all *threo* and *erythro* isomers.[18−20] Recently, Duan et al. reported the isolation of the individual isomers of a structurally related compound, NSC23925 ([2-(4-methoxyphenyl)quinolin-4-yl]-(piperidin-2-yl)methanol), through synthesis and subsequent chromatographic purification.[31] We modified and employed a synthetic approach recently presented by León[32] to access novel racemic Vacquinol analogs (Scheme 1A). Briefly, regioselective activation of 2,4-dibromoquinoline at the 4-position using *i*PrMgCl·LiCl complex generated a Grignard intermediate which, upon reaction with racemic *tert*-butyl 2-formylpiperidine-1-carboxylate resulted in nonspecific *syn* and *anti*-addition to yield 2-bromoquinoline **4**, comprising all *threo* and *erythro* isomers. Subsequent Suzuki coupling at the 2-bromo position of the quinoline utilizing aryl boronic acids or esters and concomitant HCl-mediated Boc-deprotection of the resulting 2-aryl intermediates yielded the desired heteroaryl Vacquinol derivatives **5**−**10** as dihydrochloride salts in 8−36% overall yield (Scheme 1A); the thiophenyl derivative **5** showing the most promising in vitro activity on U3013 glioma cell[33] viability (Table 1).

As the *erythro* isomers were of primary interest, intermediate **4** was purified by conventional chromatography to obtain the *erythro* racemate **11** for further elaboration (Scheme 1A). Suzuki coupling of **11**, as described above with boronic acids or esters in the presence of $Pd(PPh_3)_4$ or $PdCl_2$(dppf), and subsequent acid-catalyzed Boc-deprotection yielded *erythro* derivatives **12**−**15** in 31−58% yield as racemic mixtures (Table 2). While the 4-trifluoromethylphenyl analog **14**

DOI: 10.1021/acs.jmedchem.6b01009
J. Med. Chem. 2016, 59, 8577−8592

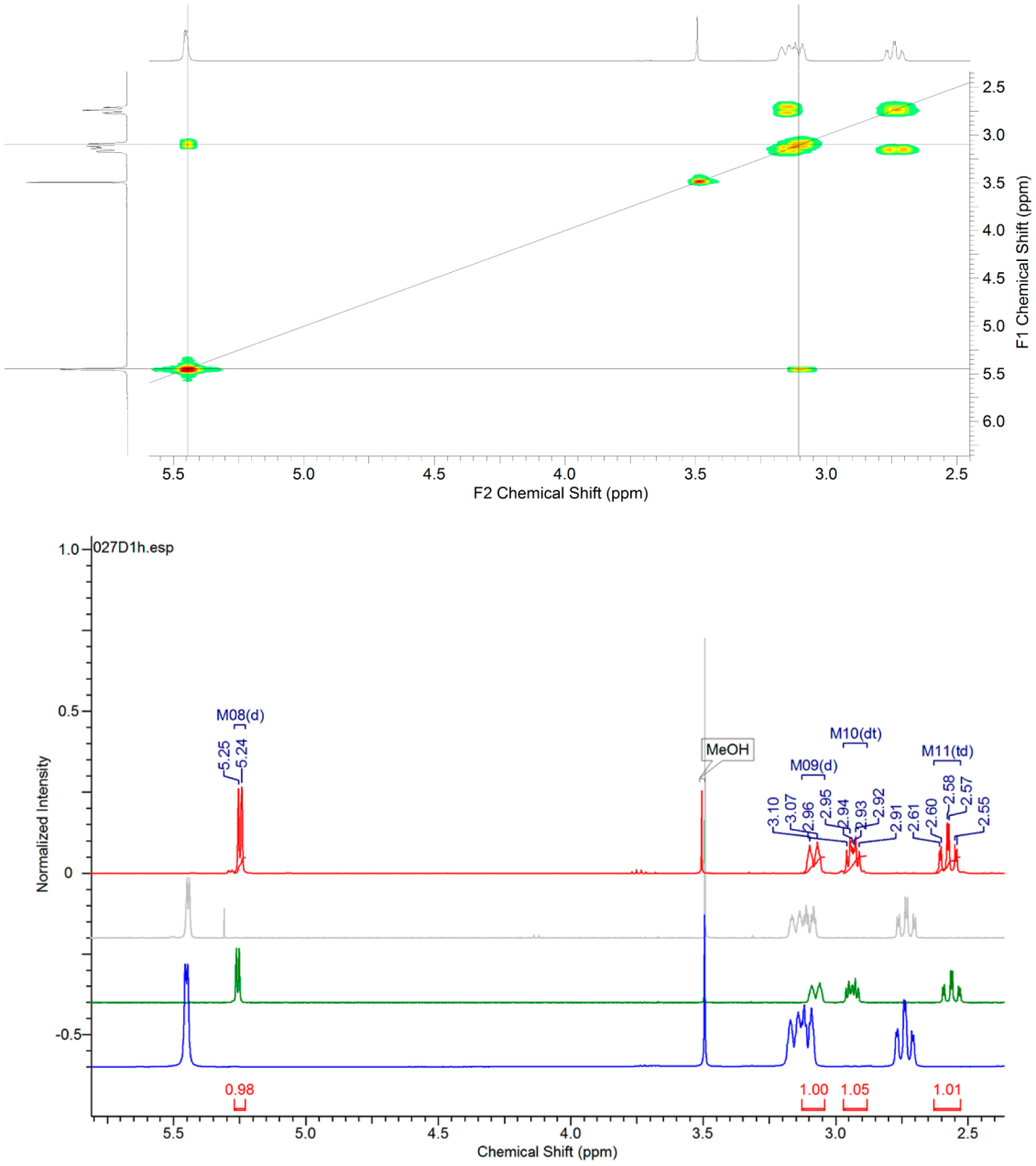

Figure 5. Top: COSY ^{1}H NMR spectrum of fraction *IIa* ([*R*,*S*]**2**) in region δ 2.4−5.5 showing coupling of C−H protons at C16 and C17. Bottom: ^{1}H NMR data of HPLC fractions *IIa* (blue), *IIb* (gray), *Ia* (green), and *Ib* (red) in the region δ 2.4−5.5 ppm (bottom). Shifts and coupling constants of the protons in enantiotopic positions C16 (δ 5.25 ppm [d, ^{3}J = 4.6 Hz] for *Ia* and *Ib*; δ 5.45 ppm (d, ^{3}J = 3.5 Hz) for *IIa* and *IIb*), and C17 (δ 2.93 ppm for *Ia* and *Ib*; δ 3.10 ppm for *IIa* and *IIb*) indicate the enantiomeric relationship of these compounds and allow for identification of *threo* vs *erythro* stereochemistry.

resulted in moderate oncolytic activity in vitro (IC_{50} = 13.5 μM) on patient-derived U3013 GBM cells, compounds **12**, **13**, and **15** were less potent.

Syntheses of Isomers of 1. Utilizing optically pure, (*S*)- or (*R*)- *tert*-butyl 2-formylpiperidine-1-carboxylates as described by Balboni et al.,[34] a synthesis was designed for generating [*R*,*S*]**2** and [*S*,*S*]**3** (via *tert*-butyl (2*S*)-2-formylpiperidine-1-carboxylate) and for generating [*S*,*R*]**2** and [*R*,*R*]**3** (via *tert*-butyl (2*R*)-2-formylpiperidine-1-carboxylate) (see Scheme 1B,C). As the resulting product mixtures from these reactions were diastereomeric in nature, the individual isomers could be separated by conventional chromatography. Polarimetry and ^{1}H NMR spectroscopic comparison of the resulting [*R*,*S*]**2** and [*S*,*R*]**2** compounds from these syntheses with spectra obtained from chromatographic fractions, whose stereochemistry had been elucidated, confirmed the stereochemistry of isolated products. In addition, analytical HPLC-MS analysis on a chiral column confirmed identity and purity (Figure S6).

The lack of stereoselectivity in the nucleophilic addition of the 2,4-dibromoquinoline Grignard intermediate to optically pure *tert*-butyl 2-formylpiperidine-1-carboxylates (Scheme 1, panels B and C) stems from the relatively minor steric contributions of the Boc group in promoting face selective addition to the aldehyde, resulting in both the *threo* and *erythro* addition products. In contrast, utilization of the corresponding 2-formylpiperidines protected with the Tr group (**19** and **23**,

DOI: 10.1021/acs.jmedchem.6b01009
J. Med. Chem. 2016, 59, 8577−8592

Scheme 1. (A) General Procedure[a] for the Non-Stereoselective Synthesis of Vacquinols 1, 5−10 and *erythro* Analogs 12−15, (B) Diastereoselective Synthesis of [*R*,*S*]2 and [*S*,*S*]3 via Optically Pure *tert*-Butyl (2*S*)-2-Formylpiperidine-1-carboxylate, and (C) Synthesis of [*S*,*R*]2 and [*R*,*R*]3 Using the Corresponding *tert*-Butyl (2*R*)-2-Formylpiperidine-1-carboxylate

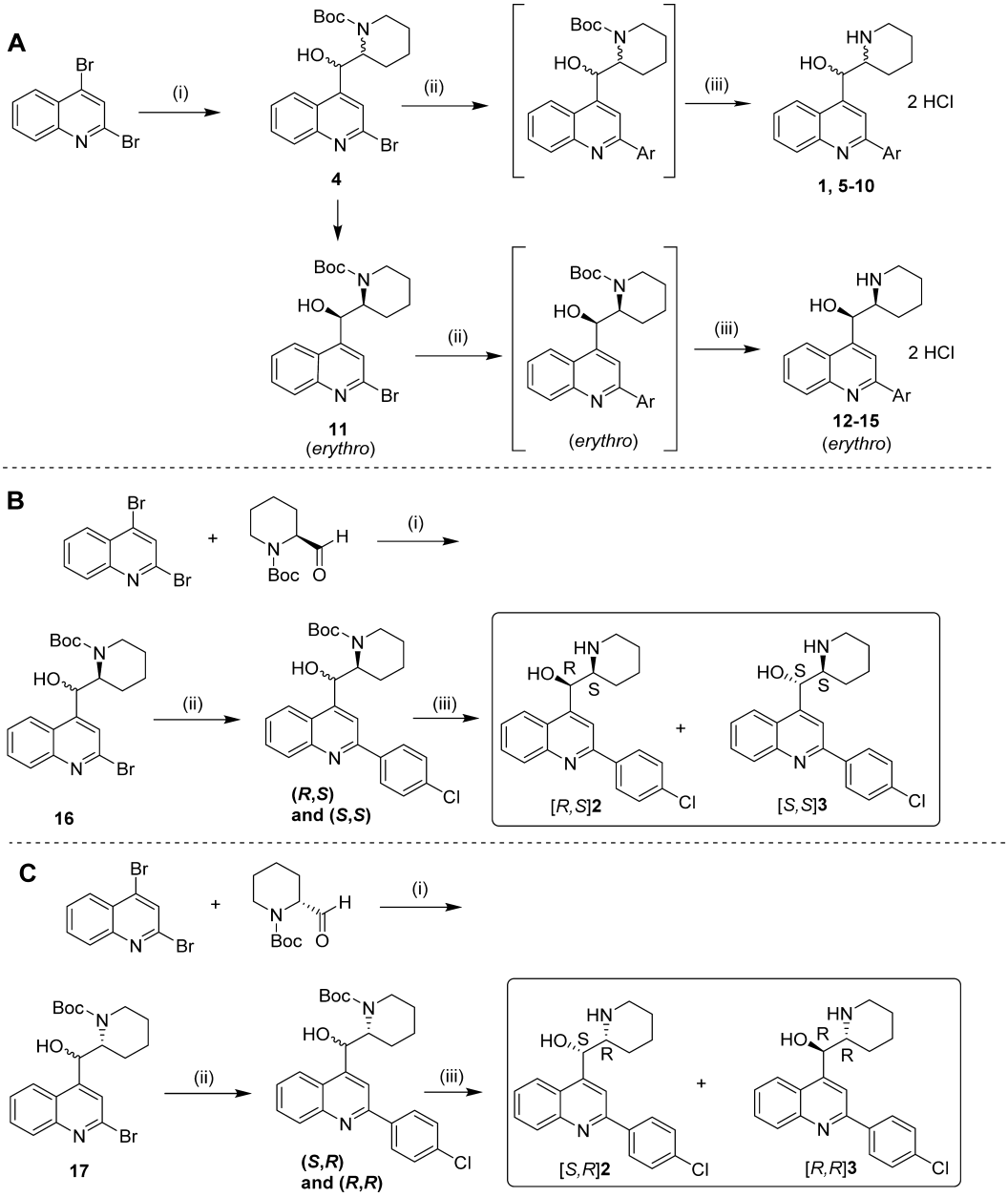

[a]General conditions: (i) *i*Pr-MgCl-LiCl (1.3 M in THF, 0−20 °C), then racemic *tert*-butyl 2-formylpiperidine-1-carboxylate (A), *tert*-butyl (2*S*)-2-formylpiperidine-1-carboxylate[34] (B), or *tert*-butyl (2*R*)-2-formylpiperidine-1-carboxylate[34] (C). (ii) arylboronic acid, $PdCl_2$(dppf) or $Pd(PPh_3)_4$, DMF, K_2CO_3, 12 h, 90 °C. (iii) HCl, Et_2O, MeOH, 0 °C (optionally work up under alkaline conditions to yield the corresponding free amine).

Scheme 2), as described by León et al.,[32] provides greater steric bulk in proximity to the aldehyde carbonyl to promote a more selective addition of the Grignard intermediate, resulting in a 90+% excess of the *erythro* addition products. This synthesis allowed for stereoselective synthesis of both [*R*,*S*]**2** and [*S*,*R*]**2** in 59−63% overall yield.

The intrinsic stereoselectivity of the reactions indicates >90% ee of the correct stereoisomer as determined by analytical HPLC using a chiral column (Figure S7). Analysis indicates 5−10% formation of the *threo* addition product, resulting from addition of the Grignard intermediate to the more sterically hindered face of trityl-protected aldehydes **19** and **23**, which can be readily removed chromatographically (Figure S8). Importantly, these results show that there is no epimerization of intermediates **19** and **23** under the basic conditions of the Grignard reaction and that the only other isomers formed are diastereomeric in nature, allowing for purification under standard conditions and confirmation of the stereochemistry of fractions isolated from chiral chromatography.

Again, comparison of NMR data from isolated fractions *IIa* and *IIb*, as well as polarimetry and retention times compared to chromatographically purified material, confirmed the identity and enantiomeric purity of [*R*,*S*]**2** and [*S*,*R*]**2** from this synthesis.

DOI: 10.1021/acs.jmedchem.6b01009
J. Med. Chem. 2016, 59, 8577−8592

Table 1. Efficiency of Suzuki Coupling and Concomitant Boc-Deprotection To Yield 2-Heteroaryl Vacquinol Analogs 5−10 and Their Corresponding in Vitro Oncolytic Activity Against U3013 Glioma Cells Compared to 1

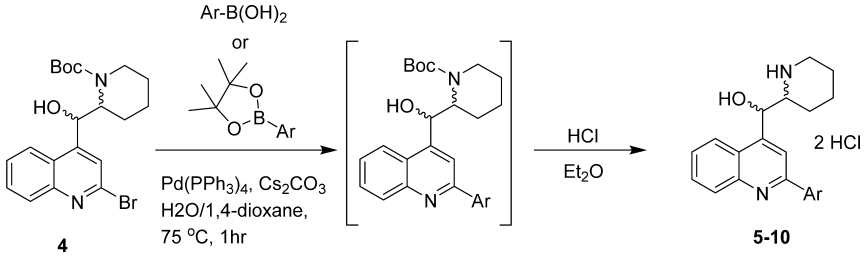

Compound	-Ar	Yield	IC_{50} (μM, U3013)[a]
1	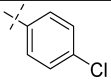	-	3.14[b]
5		77%	26.5
6	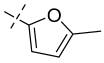	88%	>50
7		50%	>50
8		62%	>50
9		68%	>50
10		33%	>50

[a]IC_{50} values are expressed as curve-fit regressions based on averages of quadruplicate measurements at each concentration. [b]As previously reported.[17]

Table 2. Efficiency of Suzuki Coupling and Concomitant HCl-Mediated Deprotection To Yield *erythro* 2-Aryl Vacquinol Analogs 12−15 and Their Corresponding in Vitro Oncolytic Activity Against U3013 Glioma Cells Compared to 1

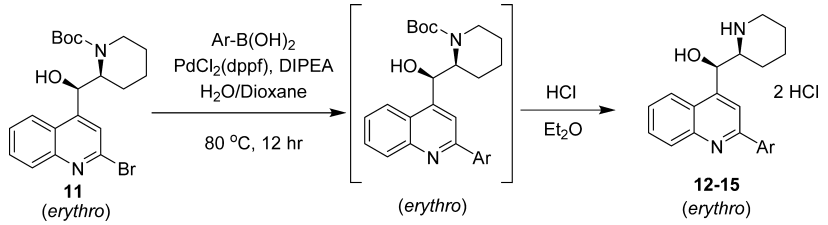

Compound	-Ar	Yield	IC_{50} (μM, U3013)[a]
1	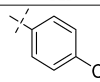	-	3.14[b]
12	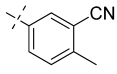	42%	32.1
13	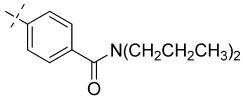	58%	35.4
14	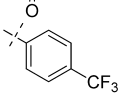	31%	13.5
15	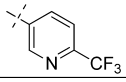	50%	38.0

[a]IC_{50} values are expressed as curve-fit regressions based on averages of quadruplicate measurements at each concentration. [b]As previously reported.[17]

(*R*)-[2-(4-Chlorophenyl)quinolin-4-yl](2*S*)-piperidin-2-ylmethanol ([*R*,*S*]2) Displays Selective Pharmacokinetic Distribution to Brain Tissue. Based on the superior in vitro activity of [*R*,*S*]**2** and [*S*,*R*]**2**, and with methods to access these

DOI: 10.1021/acs.jmedchem.6b01009
J. Med. Chem. 2016, 59, 8577−8592

Scheme 2. Stereoselective Synthesis[a] of [*R*,*S*]2 and [*S*,*R*]2 via *N*-Trityl-Protected (*S*)-Piperidine-2-carbaldehyde 19 (A) and (*R*)-Piperidine-2-carbaldehyde 23 (B)

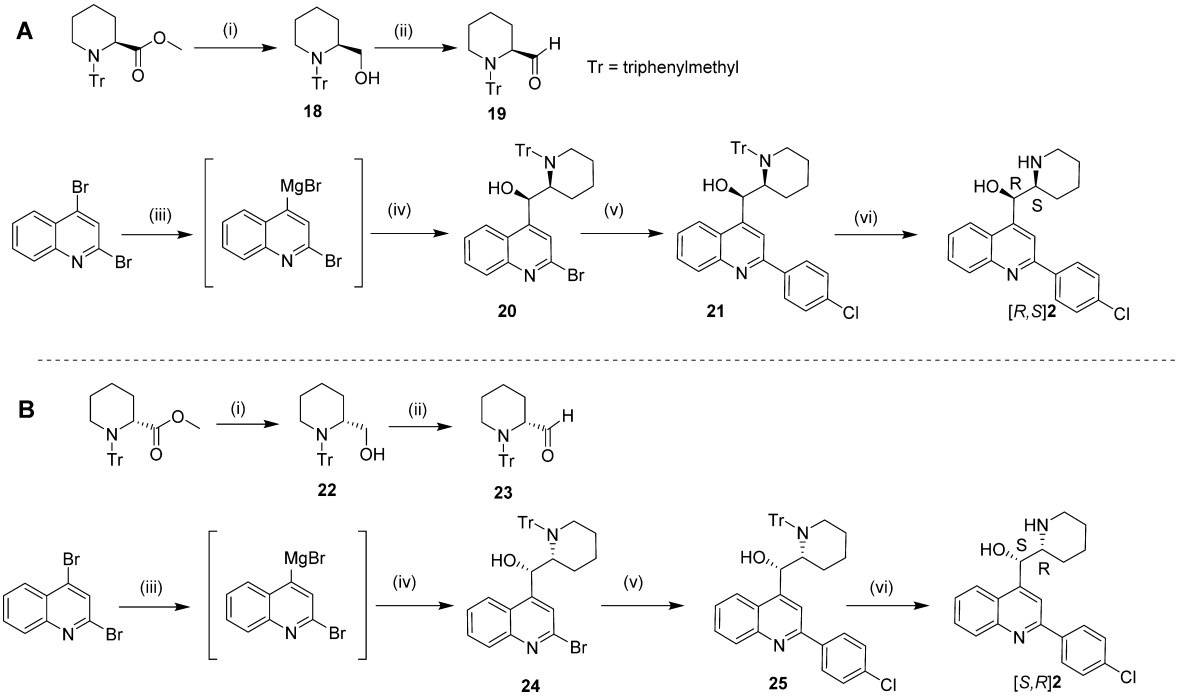

[a]General reagents and conditions: (i) $LiAlH_4$, THF, rt, 3 h. (ii) (a) Oxalyl chloride, DMSO, DCM, −78 °C, 2 h, (b) TEA, NH_4Cl. (iii) *i*PrMgCl·LiCl, THF, −5 °C to rt, 20 min. (iv) **19** or **23**, rt, 5 h. (v) 4-Chlorophenylboronic acid, $PdCl_2$(dppf), 2-MeTHF, 80 °C, 5 h. (vi) (a) HCl, Et_2O, rt, 4 h, (b) NaOH, DCM.

Table 3. Summarized Pharmacokinetic Parameters after Administration of 2 mg/kg (i.v.) or 20 mg/kg (p.o.) [*R*,*S*]2 and [*S*,*R*]2 to NMRI Mice

		tissue										
		brain						plasma				
	dose (mg/kg)	C_{max} (ng/mL)	t_{max} (h)	AUC_{last} (h × ng/mL)	t_{last} (h)	$t_{1/2}$ (h)	*F* (%)	C_{max} (ng/mL)	t_{max} (h)	AUC_{last} (h × ng/mL)	t_{last} (h)	$t_{1/2}$ (h)
[*R*,*S*]2	2 (i.v.)	1970	0.25	53100	144	72	–	775	4.0	62000	144	84
[*S*,*R*]2	2 (i.v.)	777	1.0	12200	144	67	–	455	0.50	14100	144	48
[*R*,*S*]2	20 (p.o.)	4840	8.0	400000	144	65	75.2	2210	4.0	246000	144	81
[*S*,*R*]2	20 (p.o.)	1490	6.0	157000	144	96	89	2050	8.0	183000	144	69

compounds on gram-scale, we next compared the in vivo pharmacokinetic properties of these isomers in mouse plasma and brain tissue to assess any potential differences in oral bioavailability, exposure, and tissue distribution. Male NMRI mice were administered a single dose of [*R*,*S*]**2** or [*S*,*R*]**2** (prepared synthetically according to Scheme 2) orally (20 mg/kg) or intravenously (i.v., 2 mg/kg), and the animals were subject to blood and brain tissue sampling at 0.25, 0.5, 1, 2, 4, 6, 8, 24, 48, 72, and 144 h (n = 3/time point) after administration. Quantification of plasma and brain levels of [*R*,*S*]**2** and [*S*,*R*]**2** was assessed using UPLC-MS/MS with an internal standard (see Experimental Section). The administered doses were well tolerated and showed no signs of inducing systemic or CNS toxicity. The in vivo exposure profiles of both [*R*,*S*]**2** and [*S*,*R*]**2** indicated slow oral absorption, rapid distribution to the brain, long elimination half-lives, and high oral bioavailability when compared to i.v. administration (see Table 3).

Surprisingly, while both isomers showed relatively equal plasma exposure, similar to the levels previously reported for **1**,[17] [*R*,*S*]**2** showed dramatically greater distribution to the brain than [*S*,*R*]**2** (Figure 6). Efficient BBB penetration is a major obstacle in the development of treatments for GBM and many compounds which are efficacious in vitro fail to affect orthotopic tumor development in vivo due to poor BBB penetration. The precise mechanism by which [*R*,*S*]**2** more efficiently penetrates into brain tissue is unknown but may partially be due to the marginally lower plasma protein binding of [*R*,*S*]**2** (f_u = 1.37%) versus [*S*,*R*]**2** (f_u = 0.59%) in mouse plasma, which may affect BBB exposure. These results indicate that the use of [*R*,*S*]**2** is superior to the use of the other isomers in terms of potency and phenotypic induction on U3013 glioblastoma cells as well as mouse brain exposure in murine models of GBM.

(*R*)-[2-(4-Chlorophenyl)quinolin-4-yl](2*S*)-piperidin-2-ylmethanol ([*R*,*S*]2) Efficiently and Selectively Depletes Human Patient-Derived Glioblastoma Cells in Vivo without Overt Toxicity. We next sought to establish the in vivo toxicity and efficacy of [*R*,*S*]**2** using a zebrafish model. This model has previously been used to assess toxicity and in vivo effect and has been shown to be predictive of efficacy in murine

DOI: 10.1021/acs.jmedchem.6b01009
J. Med. Chem. 2016, 59, 8577−8592

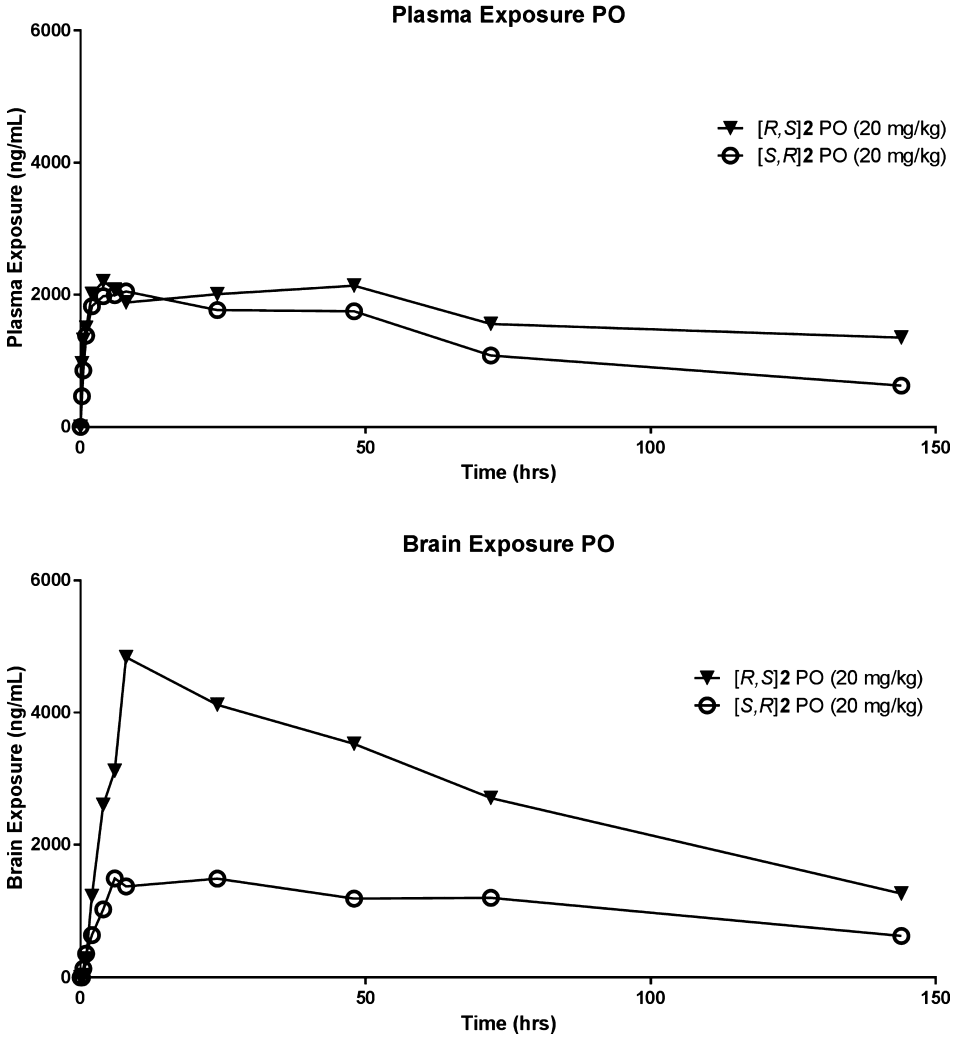

Figure 6. In vivo pharmacokinetic profiles of [*R*,*S*]**2** and [*S*,*R*]**2** in mouse plasma (top) and mouse brain tissue (bottom) after a single oral (20 mg/kg) dose, indicating enantiospecific tissue distribution profiles. Individual data points are expressed as mean values of three individual measurements.

orthotopic models of GBM.[35,36] First, zebrafish embryos were exposed to increasing concentrations of [*R*,*S*]**2** (prepared synthetically according to Scheme 2) or vehicle. The effects on zebrafish larval development was recorded at 2 days post-fertilization. No visible toxicity was seen on zebrafish development, even at the highest tested concentration of 50 μM, indicating that the compounds were well tolerated and did not hinder normal development (Figure 7).

The in vivo efficacy of [*R*,*S*]**2** was next evaluated. U3013 human glioma cells labeled with Cell Tracker Green were transplanted into the ventricles of 2 days post-fertilization zebrafish larvae and exposed to [*R*,*S*]**2** or vehicle (0.1% DMSO). The larvae were imaged 6 days post-transplantation, and fluorescence intensity quantified to evaluate tumor burden (Figure 7). 89 out of 94 animals treated with vehicle in the aquarium water revealed clear dispersion of human tumors, often arising at multiple sites and most prominently in ventricles. Only 3 out of a total of 38 analyzed animals displayed any overt presence of grafted tumor cells when treated with 30 μM [*R*,*S*]**2**. Quantification of fluorescence intensity confirmed the robust in vivo effect (Figure 7). These data show that [*R*,*S*]**2** effectively reduced human tumor cells in vivo without significant risks of defects to the larvae.

CONCLUSIONS

Novel treatments for GBM are desperately needed. Catastrophic vacuolization induced by **1** presents a conceptually new mechanism to selectively target GBM cells and may be a promising new experimental therapeutic for treating GBM. We have undertaken a systematic evaluation of the stereochemical effects elicited by the individual isomers of **1** on oncolytic in vitro efficacy against human glioma cells and pharmacokinetic distribution in vivo. The results show that the *erythro* isomers [*R*,*S*]**2** and [*S*,*R*]**2** are superior to the corresponding *threo* isomers in terms of in vitro potency. In addition, we show a stereospecificity between the individual *erythro* isomers in terms of their in vivo distribution in tissue. While [*S*,*R*]**2** shows approximately equal distribution into plasma and brain tissue, [*R*,*S*]**2** shows over 2-fold greater exposure to mouse brain tissue compared to plasma. Isomer [*R*,*S*]**2** efficiently depletes human glioblastoma cells in an orthotopic in vivo zebrafish xenograft model of GBM. As in vitro potency, selectivity, CNS exposure, and in vivo efficacy are all critical for therapeutic effect in the clinical setting, our data indicate that [*R*,*S*]**2** is a promising lead for further development. We have designed a series of stereoselective syntheses of Vacquinol analogs, allowing direct access to the individual isomers of **1** and other analogs in this

DOI: 10.1021/acs.jmedchem.6b01009
J. Med. Chem. 2016, 59, 8577−8592

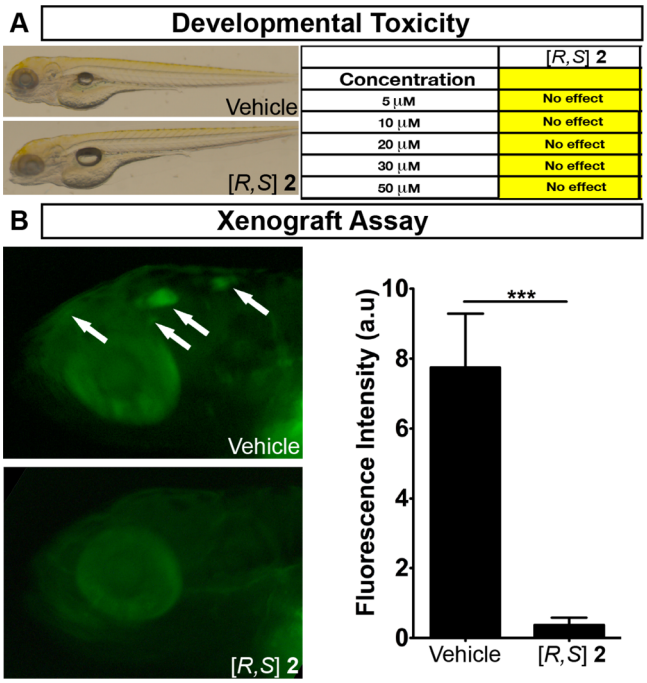

Figure 7. (A) Assessment of in vivo developmental toxicity of [*R,S*]**2** on zebrafish embryos. No observable toxicity was observed at any tested concentration up to 50 μM. (B) in vivo therapeutic efficacy assessment of [*R,S*]**2** at 30 μM concentrations in an orthotopic xenograft model of GBM in zebrafish. Arrows denote areas of U3013 GBM tumor development. Graph shows quantification of the GFP intensity of the xenografted animals treated with [*R,S*]**2** vs vehicle.

series for continued evaluation as experimental therapeutics for the treatment of GBM.

EXPERIMENTAL SECTION

General. Unless otherwise noted, all solvents and reagents were obtained from commercial sources and used without further purification or characterization. All reactions involving air- or moisture-sensitive reagents were performed under a nitrogen atmosphere using oven-dried glassware. THF, DCM, toluene, and diethyl ether were either obtained from commercial source or dried by refluxing on sodium metal and freshly distilled as per requirement. Unless otherwise indicated, all reactions were performed at ambient temperatures (18−25 °C). Microwave-assisted reactions were performed using a Biotage Initiator. Reactions were magnetically stirred and monitored by thin-layer chromatography using TLC silica gel 60 F 254 aluminum sheets from Merck and analyzed with 254 nm UV light, iodine stain, or ninhydrin. Flash chromatography was performed with silica gel from Merck (60−120 mesh, pH = 6.5−7.5). Preparative HPLC was performed on a Gilson 305 HPLC system using either a basic (Xbridge C18 (5 μm, 30 × 75 mm) column using a gradient system of acetonitrile and H_2O containing 50 mM NH_4HCO_3, pH 10) or an acidic (ACE 5 C8 (5 μm, 30 × 150 mm) column using a gradient system of acetonitrile and H_2O containing 0.1% TFA) eluting protocol at a 25 mL/min flow rate. Alternatively, HPLC was performed on a Knauer preparative LC system consisting of preparative K-1800 pumps, preparative dynamic mixing chamber, a UV detector K-2501 set at 265 nm, and a 765 Dosimat injection pump (Metrohm) using a 20 mL injection loop. The instrument system was controlled by software EZChromElite 3.1.3. The column was a Kromasil Silica (100 A) 10 μm, 50 × 190 mm and was held at an ambient temperature. The eluent was a 50/50 mixture of ethanol (99.7%, Solveco) and *n*-heptane (Fraction HPLC, LabScan) with a 0.2% diethyl amine (puriss, Sigma-Aldrich) additive in both phases, pumped at a flow rate of 100 mL/min. Unless other conditions are specified, chiral preparative chromatography was achieved on a Waters auto semipurification system equipped with an 2767 auto sampler-combined automated fraction collector, 2525 gradient pump, 600 regeneration pump, 515 make-up pump, CFO column switch, and 2996 PDA spectrometer scanning at 210−350 nm. The system was controlled by Waters MassLynx V 4.1 and by FractionLynx. Nuclear magnetic resonance (^{1}H and ^{13}C NMR) spectra were recorded using an internal deuterium lock at ambient temperature on a Bruker Avance-III 500 MHz system using Topspin-3 software or a Bruker Avance-II DPX 400 MHz system using Topspin-1 software. All final compounds were purified to ≥95% purity as determined by LC-MS or HPLC/UPLC and ^{1}H NMR. Polarimetry was performed on a Rudolph Autopol II fitted with a tungsten halogen lamp measuring at 589 nm (sodium line-D) using a 0.7 mL cuvette with 30 mm path length. Before each measurement, a blank sample (cell with pure solvent) was used to zero the instrument.

Chromatographic Purification of Isomers. Compound **1** was prepared as previously reported,[17] and injections of 45 mg (in 10 mL ethanol) of the racemic material were purified using a Knauer preparative chromatography system (see Generalsection for details). Fractions were collected manually, determined by UV monitoring at 265 nm. Obtained enantiomer fractions *I* and *II* (see Figure 2) were concentrated in vacuo for further separation on HPLC using chiral columns.

Chiral separation of fraction *I* was performed on a Chiralcel OD-H 5 μm 20 × 250 mm column held at 22 °C and eluted with a 1:9 mixture of ethanol and *n*-heptane with a 0.2% diethyl amine additive to both phases. The eluent was pumped at a flow rate of 20 mL/min. Injections of 2 mg (in 0.5 mL of ethanol) were made. Fractions were collected by PDA detector triggering on the isomers UV signals. The enantiomerically pure fractions *Ia* (35 mg) and *Ib* (25 mg) were obtained upon evaporation of solvent.

Chiral separation of fraction *II* was performed over a Chiralpak AD-H 5 μm 20 × 250 mm column held at 35 °C and eluted with a 3:7 mixture of ethanol and *n*-heptane with a 0.2% diethyl amine additive to both phases. The eluent was pumped at a flow rate of 20 mL/min. Injections of 4.5 mg (in 1 mL of ethanol) were made. Fractions were collected by PDA detector triggering on the isomers UV signals. The enantiomerically pure fractions *IIa* (49 mg) and *IIb* (48 mg) were obtained upon evaporation of solvent.

All obtained fractions were analyzed for chiral and chemical purity on a Dionex Summit HPLC system consisting of a pump, a temperature-controlled automated sampler, a column compartment, and a UVD340U UV detector. The UV was recorded at 265 nm wavelength. The instrument system was controlled by Chromeleon v6.0 software. The columns and mobile phases used were as reported for the respective preparative systems, except that the column sizes were 4.6 × 250 mm, the diethyl amine addition to each mobile phase was 0.1%, and the flow rate was 1 mL/min.

Analytical Data for Isomers of ***1****. Compound [R,S]****2*** *(Fraction IIa).* $[\alpha]_D^{25}$ = +14.1 (*c* 0.7, $CHCl_3$). ^{1}H NMR (400 MHz, $CDCl_3$) δ 8.19 (dd, *J* = 1.1, 8.7 Hz, 1H), 8.16 (d, *J* = 8.5 Hz, 2H), 8.10 (s, 1H), 7.93 (dd, *J* = 0.6, 8.5 Hz, 1H), 7.72 (ddd, *J* = 1.3, 7.0, 8.5 Hz, 1H), 7.50−7.54 (m, 1H), 7.49 (d, *J* = 8.5 Hz, 2H), 5.45 (d, *J* = 3.5 Hz, 1H), 3.15 (td, *J* = 1.9, 11.8 Hz, 1H), 3.10 (td, *J* = 3.0, 11.4 Hz, 1H), 2.74 (dt, *J* = 2.7, 11.9 Hz, 1H), 1.72 (d, *J* = 12.6 Hz, 1H), 1.57 (d, *J* = 13.3 Hz, 1H), 1.29−1.46 (m, 2H), 1.06−1.22 (m, 2H). ^{13}C NMR (101 MHz, $CDCl_3$) δ 155.7, 148.3, 147.2, 138.1, 135.5, 130.6, 129.3, 128.9, 128.9, 126.3, 124.7, 122.7, 116.0, 72.5, 59.9, 46.9, 26.0, 25.0, 23.9. LC-MS (API-ES) *m/z*: 353 $[M + H]^+$.

*Compound [S,R]****2*** *(Fraction IIb).* $[\alpha]_D^{25}$ = −14.3 (*c* 0.4, $CHCl_3$). ^{1}H NMR (400 MHz, $CDCl_3$) 8.19 (dd, *J* = 1.1, 8.7 Hz, 1H), 8.16 (d, *J* = 8.5 Hz, 2H), 8.10 (s, 1H), 7.93 (dd, *J* = 0.6, 8.5 Hz, 1H), 7.72 (ddd, *J* = 1.3, 7.0, 8.5 Hz, 1H), 7.50−7.54 (m, 1H), 7.49 (d, *J* = 8.5 Hz, 2H), 5.44 (d, *J* = 3.5 Hz, 1H), 3.15 (td, *J* = 1.9, 11.8 Hz, 1H), 3.10 (td, *J* = 3.0, 11.4 Hz, 1H), 2.73 (dt, *J* = 2.8, 12.0 Hz, 1H), 1.72 (d, *J* = 12.6 Hz, 1H), 1.57 (d, *J* = 13.3 Hz, 1H), 1.29−1.44 (m, 2H), 1.06−1.21 (m, 2H). ^{13}C NMR (101 MHz, $CDCl_3$) δ 155.7, 148.3, 147.3, 138.1, 135.5, 130.6, 129.3, 128.9, 128.9, 126.3, 124.7, 122.7, 116.0, 72.5, 59.9, 46.9, 26.0, 25.0, 23.9. LC-MS (API-ES) *m/z*: 353 $[M + H]^+$.

DOI: 10.1021/acs.jmedchem.6b01009
J. Med. Chem. 2016, 59, 8577−8592

*Compound [R,R]**3** (Fraction Ia).* $[\alpha]_D^{25}$ = +19.3 (*c* 0.7, $CHCl_3$). ^1H NMR (400 MHz, $CDCl_3$) δ 8.18−8.22 (m, 1H), 8.14−8.18 (m, 2H), 8.02 (s, 1H), 7.95 (dd, *J* = 0.6, 8.5 Hz, 1H), 7.74 (ddd, *J* = 1.3, 7.0, 8.5 Hz, 1H), 7.55 (ddd, *J* = 1.4, 6.9, 8.4 Hz, 1H), 7.48−7.52 (m, 2H), 5.26 (d, *J* = 4.4 Hz, 1H), 3.08 (d, *J* = 12.0 Hz, 1H), 2.90−2.98 (m, 1H), 2.56 (dt, *J* = 2.7, 11.8 Hz, 1H), 1.76−1.85 (m, 1H), 1.50−1.64 (m, 3H), 1.42 (td, *J* = 3.7, 12.2 Hz, 1H), 1.21−1.35 (m, 1H). ^{13}C NMR (101 MHz, $CDCl_3$) δ 155.6, 149.0, 148.4, 137.9, 135.6, 130.6, 129.5, 129.0, 128.8, 126.4, 125.0, 122.9, 115.7, 72.5, 61.0, 46.2, 29.4, 25.9, 24.2. LC-MS (API-ES) *m*/*z*: 353 $[M + H]^+$.

*Compound [S,S]**3** (Fraction Ib).* $[\alpha]_D^{25}$ = −18.9 (*c* 0.8, $CHCl_3$). ^1H NMR (400 MHz, $CDCl_3$) δ 8.21 (dd, *J* = 1.0, 8.5 Hz, 1H), 8.12−8.18 (m, 2H), 8.01 (s, 1H), 7.95 (dd, *J* = 0.9, 8.5 Hz, 1H), 7.75 (ddd, *J* = 1.3, 6.8, 8.4 Hz, 1H), 7.52−7.57 (m, 1H), 7.48−7.52 (m, 2H), 5.25 (d, *J* = 4.7 Hz, 1H), 3.08 (d, *J* = 11.7 Hz, 1H), 2.93 (td, *J* = 5.2, 8.3 Hz, 1H), 2.58 (dt, *J* = 2.8, 11.9 Hz, 1H), 1.79 (td, *J* = 1.6, 13.0 Hz, 1H), 1.50−1.64 (m, 3H), 1.36−1.50 (m, 1H), 1.21−1.35 (m, 1H). ^{13}C NMR (101 MHz, $CDCl_3$) δ 155.6, 149.0, 148.4, 137.9, 135.6, 130.6, 129.5, 129.0, 128.8, 126.4, 125.0, 122.9, 115.7, 72.5, 61.0, 46.2, 29.4, 25.9, 24.2. LC-MS (API-ES) *m*/*z*: 353 $[M + H]^+$.

Chemistry. *(R)-[2-(4-Chlorophenyl)quinolin-4-yl](2S)-piperidin-2-ylmethanol ([R,S]**2**) and (S)-[2-(4-Chlorophenyl)quinolin-4-yl]-(2S)-piperidin-2-ylmethanol ([S,S]**3**) from **16**.* Compound **16** (139 mg, 0.33 mmol) and 4-chlorophenylboronic acid (62 mg, 0.4 mmol) were dissolved in 2-methyltetrahydrofuran (2 mL) under N_2, and $PdCl_2$(dppf) (2.7 mg, 0.03 mmol) and 2 M aqueous K_2CO_3 (0.49 mL, 1.0 mmol) were added under nitrogen atmosphere, and the reaction was heated at 90 °C overnight. The mixture was purified by silica gel flash chromatography (ethyl acetate/heptane, 1:3) and dried under vacuum, yielding the Boc-protected intermediates *tert*-butyl (2*S*)-2-[(*R*)-[2-(4-chlorophenyl)quinolin-4-yl (hydroxy)methyl]piperidine-1-carboxylate and *tert*-butyl (2*S*)-2-[(*S*)-[2-(4-chlorophenyl)quinolin-4-yl (hydroxy)methyl]piperidine-1-carboxylate as white solids. LC-MS (API-ES) *m*/*z*: 453 $[M + H]^+$. The material was dissolved in MeOH (1 mL) and cooled to 0 °C. A solution of HCl 1 M in diethyl ether (1.45 mL, 1.45 mmol) was added, and the solution was allowed to warm to rt overnight. The formed precipitate was filtered and dried under vacuum to give crude product (68 mg with HPLC purity 85%). The crude material was dissolved in acetonitrile (2 mL) and 25% aqueous ammonia (1 mL), and the individual isomers purified by preparatory HPLC to give title compounds [*R*,*S*]**2** (42.5 mg, 50%) and [*S*,*S*]**3** (28.5 mg, 54%) as white solids. NMR, optical rotation, and chiral analytical LCMS retention times matched data provided for [*R*,*S*]**2** and [*S*,*S*]**3** from chromatographic purification (fractions *IIa* and *Ib*, respectively).

*(R)-[2-(4-Chlorophenyl)quinolin-4-yl](2S)-piperidin-2-ylmethanol ([R,S]**2**) from **21**.* (*R*)-[2-(4-Chlorophenyl)quinolin-4-yl][(2*S*)-1-(triphenylmethyl)piperidin-2-yl]methanol (**21**) (810 mg, 1.36 mmol) was dissolved in diethyl ether (46 mL), followed by addition of 5 M aqueous HCl (5.7 mL). After stirring at rt for 4 h, the solution was partitioned between diethyl ether (60 mL) and H_2O (60 mL). The aqueous layer was extracted with diethyl ether (3 × 50 mL). The aqueous layer was then alkalinized with 6 M aqueous NaOH and extracted with DCM (50 mL). The organic fraction was dried over $MgSO_4$, filtered, and concentrated in vacuo. Purification by flash chromatography (TEA/MeOH/DCM, 1:1:98) yielded the crude product (280 mg, 60%) as an off-white solid. The material was purified by preparative HPLC under acidic conditions. The pure fraction was collected and concentrated under reduced pressure, the pH was adjusted to 10 using 1 M NaOH, followed by extraction with DCM (3 × 50 mL). The combined organic layers were dried over anhydrous Na_2SO_4, concentrated under reduced pressure, and recrystallized from acetone to give the title compound (265 mg, 55%) as a white solid. NMR, optical rotation, and chiral analytical LCMS retention times matched data provided for [*R*,*S*]**2** from chromatographic purification (fraction *IIa*).

*(S)-[2-(4-Chlorophenyl)quinolin-4-yl](2R)-piperidin-2-ylmethanol ([S,R]**2**) and (R)-[2-(4-Chlorophenyl)quinolin-4-yl](2R)-piperidin-2-ylmethanol ([R,R]**3**) from **17**.* Compounds [*S*,*R*]**2** and [*R*,*R*]**3** were prepared according to the same procedure as for [*R*,*S*]**2** and [*S*,*S*]**3** from **16** above but using **17** (156 mg, 0.34 mmol) as starting material to give [*S*,*R*]**2** (82 mg, 67%) and [*R*,*R*]**3** (55 mg, 48%) as white solids. NMR and chiral analytical LCMS retention times matched data provided for [*S*,*R*]**2** and [*R*,*R*]**3** from chromatographic purification (fractions *IIb* and *Ia*, respectively).

*(S)-[2-(4-Chlorophenyl)quinolin-4-yl](2R)-piperidin-2-ylmethanol ([S,R]**2**) from **25**.* The compound was prepared according to the same procedure as for [*R*,*S*]**2** from **21** but using **25** (8.5 g, 14.3 mmol) as starting material. Chromatographic purification gave the title compound (4.9 g, 88%) as a white solid. NMR, optical rotation, and chiral analytical LCMS retention times matched data provided for [*S*,*R*]**2** from chromatographic purification (fraction *IIb*).

*tert-Butyl 2-[(2-bromoquinolin-4-yl) (hydroxy)methyl]piperidine-1-carboxylate (**4**).* A dry and nitrogen-flushed flask, equipped with a magnetic stirring bar and a septum, was charged with 2,4-dibromoquinoline (500 mg, 1.74 mmol) dissolved in dry THF (6 mL). 1.3 M *i*PrMgCl·LiCl in THF (1.47 mL, 1.92 mmol) was added dropwise at rt, followed by the addition of *tert*-butyl 2-formylpiperidine-1-carboxylate (483 mg, 2.27 mmol). The mixture was stirred for 4 h. Saturated aqueous NH_4Cl solution (50 mL) was added, and the mixture was extracted with ethyl acetate (3 × 20 mL). The combined organic fractions were dried over anhydrous Na_2SO_4 and evaporated, and the product was purified by flash chromatography (ethyl acetate/heptane, 1:4) and subsequent recrystallization in methanol to afford **4** (424 mg, 58%) as a white solid containing four isomers. ^1H NMR ($CDCl_3$, 400 MHz): δ 8.22 (dd, *J* = 8.5, 0.9 Hz, 1 H), 7.97 (dd, *J* = 8.6, 0.8 Hz, 1 H), 7.62−7.73 (m, 2 H), 7.55 (ddd, *J* = 8.3, 6.9, 1.4 Hz, 1 H), 5.66 (t, *J* = 4.5 Hz, 1 H), 4.31 (q, *J* = 5.1 Hz, 1 H), 3.83 (d, *J* = 13.1 Hz, 1 H), 3.71 (br. s., 1 H), 3.19 (ddd, *J* = 14.3, 13.1, 4.0 Hz, 1 H), 1.87−1.98 (m, 1 H), 1.77 (tt, *J* = 9.5, 4.5 Hz, 1 H), 1.59 (tt, *J* = 8.1, 4.0 Hz, 1 H), 1.42−1.54 (m, 2 H), 1.21−1.41 ppm (m, 10 H). LC-MS (ESI) *m*/*z*: 421 $[M + H]^+$.

*[2-(Thiophen-3-yl)quinoline-4-yl](piperidine-2-yl)methanol Dihydrochloride (**5**).* Compound **4** (100 mg, 0.24 mmol) and 3-thiophenylboronic acid (33.8 mg, 0.26 mmol) together with $Pd(PPh_3)_4$ (27.7 mg, 0.02 mmol) and 1,4 dioxane/water (1:1, 50 mL) were charged into a 100 mL round-bottom flask. The flask was degassed with nitrogen three times. To the mixture was added Cs_2CO_3 (114 mg, 0.35 mmol), and the reaction mixture was stirred at 75 °C for 18 h. After cooling to rt, the reaction mixture was diluted with water (50 mL) and extracted with ethyl acetate (3 × 20 mL). The combined organic layers were washed with brine, dried over anhydrous $MgSO_4$, and concentrated under reduced pressure. The resulting Boc-protected intermediate was purified by column chromatography (ethyl acetate:DCM, 1:9). LC-MS (ESI) *m*/*z*: 425 $[M + H]^+$. The material was immediately dissolved in DCM (30 mL) and treated with excess 1 M HCl etherate for 6 h to precipitate the di-HCl salt. Filtration and evaporation afforded **5** as a mixture of four stereoisomers (66 mg, 77%) as a white solid. ^1H NMR (400 MHz, DMSO-d_6): δ = 8.34−8.86 (m, 3 H), 8.28 (d, *J* = 6.1 Hz, 1 H), 8.06−8.16 (m, 1 H), 7.90−8.01 (m, 1 H), 7.71−7.87 (m, 2 H), 6.07 (s, 0.45 H), 5.68 (d, *J* = 7.1 Hz, 0.55 H), 3.38−3.60 (m, 1 H), 3.27 (d, *J* = 12.1 Hz, 1 H), 2.72−3.07 (m, 1 H), 1.54−1.85 (m, 4 H), 1.18−1.51 ppm (m, 2 H). HRMS (ESI) *m*/*z*: calcd for $C_{19}H_{20}N_2OS$: 325.1369, found: 325.1366 $[M + H]^+$.

*[2-(5-Methylfuran-2-yl)quinoline-4-yl](piperidine-2-yl)methanol Dihydrochloride (**6**).* The compound was prepared according to the same procedure as **5** but using 5-methyl-2-furanboronic pinacol ester on a 100 mg (0.24 mmol) scale. The Boc-protected intermediate (LC-MS (ESI) *m*/*z*: 423 $[M + H]^+$) was purified by column chromatography (ethyl acetate/heptane, 1:3) and deprotected overnight as described for **5** to afford **6** (75 mg, 88%) as a yellow solid. ^1H NMR (400 MHz, DMSO-d_6): δ = 8.39−8.69 (m, 2 H), 8.09−8.23 (m, 1 H), 7.69−8.00 (m, 3 H), 6.55 (d, *J* = 2.5 Hz, 1 H), 6.10 (s, 0.5 H), 5.72 (d, *J* = 6.6 Hz, 0.5 H), 3.34−3.52 (m, 1 H), 3.16−3.32 (m, 1 H), 2.75−3.08 (m, 1 H), 1.18−1.88 ppm (m, 6 H). HRMS (ESI) *m*/*z* calcd for $C_{20}H_{22}N_2O_2$: 323.1749, found: 323.1754 $[M + H]^+$.

*[2-(1H-Pyrrol-2-yl)quinoline-4-yl](piperidine-2-yl)methanol Dihydrochloride (**7**).* The compound was prepared according to the same procedure as **5** but using *N*-Boc-2-pyrrolboronic acid on a 100 mg

DOI: 10.1021/acs.jmedchem.6b01009
J. Med. Chem. 2016, 59, 8577−8592

(0.24 mmol) scale. The Boc-protected intermediate (LC-MS (ESI) *m/z*: 408 $[M + H]^+$) was purified by column chromatography (ethyl acetate/DCM, 1:9) and deprotected overnight as described for **5** to afford **7** (41 mg, 50%) as a yellow solid. ^{1}H NMR (400 MHz, DMSO-d_6): δ = 12.99 (br. s., 1 H), 10.35 (d, *J* = 9.6 Hz, 0.7 H), 9.17−9.34 (m, *J* = 9.6 Hz, 0.3 H), 8.25−8.67 (m, 4 H), 7.98 (t, *J* = 7.6 Hz, 1 H), 7.73 (t, *J* = 7.6 Hz, 1 H), 7.49 (s, 1 H), 6.47 (s, 1 H), 6.02 (s, 0.7 H), 5.62 (d, *J* = 6.6 Hz, 0.3 H), 3.36−3.48 (m, 1 H), 3.25 (d, *J* = 10.6 Hz, 1 H), 2.72−3.05 (m, *J* = 11.6 Hz, 1 H), 1.49−1.84 (m, 4 H), 1.18−1.44 ppm (m, 2 H). HRMS (ESI) *m/z* calcd for $C_{19}H_{21}N_3O$: 308.1757, found: 308.1753 $[M + H]^+$.

*[2-(Pyridin-4-yl)quinoline-4-yl](piperidine-2-yl)methanol Dihydrochloride (**8**).* The compound was prepared according to the same procedure as **5** but using 4-pyridinylboronic acid on a 100 mg (0.24 mmol) scale. The Boc-protected intermediate (LC-MS (ESI) *m/z*: 420 $[M + H]^+$) was purified by column chromatography (DCM/MeOH, 95:5) and deprotected overnight as described for **5** to afford **8** (52 mg, 55%) as a white solid. ^{1}H NMR (400 MHz, DMSO-d_6): δ = 9.08 (dd, *J* = 13.1, 6.6 Hz, 2 H), 8.22−8.87 (m, 5 H), 7.71−8.00 (m, 2 H), 6.12 (s, 0.5 H), 5.74 (d, *J* = 7.6 Hz, 0.5 H), 3.18−3.62 (m, 2 H), 2.75−3.04 (m, 1 H), 1.51−1.85 (m, 4 H), 1.16−1.41 ppm (m, 2 H). HRMS (ESI) *m/z* calcd for $C_{20}H_{21}N_3$: 320.1757, found: 325.1754 $[M + H]^+$.

*[2-(Pyrimidin-5-yl)quinoline-4-yl](piperidine-2-yl)methanol Dihydrochloride (**9**).* The compound was prepared according to the same procedure as **5** but using 5- pyrimidinylboronic acid on a 100 mg (0.24 mmol) scale. The Boc-protected intermediate (LC-MS (ESI) *m/z*: 421 $[M + H]^+$) was purified by column chromatography (DCM/MeOH, 95:5) and deprotected overnight as described for **5** resulting in **9** (58 mg, 68%) as an off-white solid. ^{1}H NMR (400 MHz, MeOD-d_4): δ = 9.25−9.71 (m, 1 H), 7.86−8.95 (m, 6 H), 6.44−6.68 (m, 1 H), 5.99−6.22 (m, 0.55 H), 5.65−5.87 (m, 0.45 H), 3.35−3.75 (m, 2 H), 2.86−3.23 (m, 1 H), 1.23−2.01 ppm (m, 6 H). HRMS (ESI) *m/z* calcd for $C_{19}H_{20}N_4O$: 321.1710, found: 321.1708 $[M + H]^+$.

*[2-(3,5-Dimethylisoxazo-4-yl)quinoline-4-yl](piperidine-2-yl)-methanol Dihydrochloride (**10**).* The compound was prepared according to the same procedure as **5** but using 3,5-dimethylisoxazole-4-boronic pinacol ester on a 100 mg (0.24 mmol) scale. The Boc-protected intermediate (LC-MS (ESI) *m/z*: 438 $[M + H]^+$) was purified by column chromatography (ethyl acetate/heptane, 1:2) and deprotected overnight as described for **5** to afford **10** (29 mg, 33%) as a yellow solid. ^{1}H NMR (400 MHz, MeOD-d_4): δ = 8.52−8.80 (m, 1 H), 7.98−8.45 (m, 4 H), 6.16 (br. s., 0.55 H), 5.81 (br. s., 0.45 H), 3.35−3.81 (m, 2 H), 2.88−3.24 (m, 1 H), 2.38−2.82 (m, 6 H), 1.66−2.05 (m, 4 H), 1.30−1.65 ppm (m, 2 H). HRMS (ESI) *m/z* calcd for $C_{20}H_{23}N_3O_2$: 338.1863, found: 338.1860 $[M + H]^+$.

*(erythro) tert-Butyl 2-[(2-bromoquinolin-4-yl) (hydroxyl)methyl]-piperidine-1-carboxylate (**11**).* *tert*-Butyl 2-((2-bromoquinolin-4-yl) (hydroxyl)methyl)piperidine-1-carboxylate (**4**) (1.02 g) was purified by flash chromatography (gradient of EtOAc/*i*-hexane 1:9 to 3:7) to give two fractions, each representing a pair of enantiomers. The stereochemistry of the first eluting fraction (205 mg, 28%; white solid; LC-MS (ESI+) *m/z*: 421 $[M + H]^+$) was determined as the mixture of the *erythro* isomers ([*R*,*S*] and [*S*,*R*]) of **11** by comparison to the relative retention order of the same intermediates in the synthesis of compounds **16** and **17**. The mixture **11** was used directly in the next step.

*(erythro) 5-{4-[Hydroxyl(piperidin-2-yl)methyl]quinolin-2-yl}-2-methyl-benzonitrile Dihydrochloride (**12**).* A solution of **11** (21 mg, 0.050 mmol), 3-cyano-4-methylphenylboronic acid (10 mg, 0.062 mmol), Pd(dppf)Cl_2·CH_2Cl_2 (2.7 mg, 0.003 mmol), and DIPEA (40 μL, 0.230 mmol) in aqueous dioxane (0.55 mL, 10% H_2O) was heated at 80 °C under N_2 atmosphere for 15 h. The reaction mixture was diluted with acetonitrile, filtered, and purified by preparative reverse-phase HPLC using basic conditions. The pure fractions were combined, and the solvent was removed under reduced pressure giving a mixture of *tert*-butyl (2*R*)-2-[(*S*)-[2-(3-cyano-4-methylphenyl)quinolin-4-yl](hydroxy)methyl]piperidine-1-carboxylate and *tert*-butyl (2*S*)-2-[(*R*)-[2-(3-cyano-4-methylphenyl)quinolin-4-yl]-(hydroxy)methyl]piperidine-1-carboxylate (MS (ESI) *m/z*: 458 $[M + H]^+$). The Boc-protected intermediate (8.5 mg) was dissolved in DCM (0.5 mL). 1 M HCl in diethyl ether (1.0 mL, 1.0 mmol) was added, and the reaction mixture was stirred at rt for 24 h. The solvent was removed under reduced pressure, giving the *erythro* isomers of the title compound (**12**) as a white solid (8.2 mg, 42%). ^{1}H NMR (400 MHz, MeOD-d_4) δ ppm 8.65 (d, *J* = 7.9 Hz, 1 H) 8.50 (s, 2 H) 8.44 (d, *J* = 8.5 Hz, 1 H) 8.33 (d, *J* = 7.9 Hz, 1 H) 8.16−8.26 (m, 1 H) 7.99−8.11 (m, 1 H) 7.81 (d, *J* = 7.9 Hz, 1 H) 6.11 (s, 1 H) 3.73 (d, *J* = 11.4 Hz, 1 H) 3.47 (d, *J* = 11.1 Hz, 1 H) 3.19 (t, *J* = 12.3 Hz, 1 H) 2.72 (s, 3 H) 1.58−1.97 (m, 4 H) 1.23−1.49 (m, 2 H). LC-MS (ESI) *m/z*: 358 $[M + H]^+$.

*(erythro) 4-{4-[Hydroxy(piperidin-2-yl)methyl]quinolin-2-yl}-N,N-dipropylbenzamide Dihydrochloride (**13**).* The compound was prepared according to the same procedure as **12** using 4-(N,N-dipropylaminocarbonyl)phenyl]boronic acid (16.3 mg, 0.065 mmol) as starting material, and heating the reaction mixture for 20 h at 80 °C. Deprotection of the Boc-protected intermediate resulted in **13** as a light brown solid (14 mg, 58%). ^{1}H NMR (400 MHz, CD_3OD) δ ppm 8.55 (d, *J* = 8.5 Hz, 1 H) 8.48 (s, 1 H) 8.40 (d, *J* = 8.5 Hz, 1 H) 8.25 (d, *J* = 8.2 Hz, 2 H) 8.12−8.19 (m, 1 H) 7.97−8.04 (m, 1 H) 7.71 (d, *J* = 8.2 Hz, 2 H) 6.06 (d, *J* = 2.5 Hz, 1 H) 3.67−3.78 (m, 1 H) 3.50−3.58 (m, 2 H) 3.44−3.50 (m, 1 H) 3.24−3.29 (m, 2 H) 3.14−3.24 (m, 1 H) 1.53−1.95 (m, 8 H) 1.25−1.47 (m, 2 H) 1.03 (t, *J* = 7.4 Hz, 3 H) 0.78 (t, *J* = 7.4 Hz, 3 H). LC-MS (ESI) *m/z*: 446 $[M + H]^+$.

*(erythro) (Piperidin-2-yl){2-[4-(trifluoromethyl)phenyl]quinolin-4-yl}methanol Dihydrochloride (**14**).* The compound was prepared according to the same procedure as **12** using 4-(trifluoromethyl)-phenyl boronic acid (11 mg, 0.057 mmol) as starting material and heating the reaction mixture for 5 h at 80 °C followed by 3 days at 65 °C. Deprotection of the Boc-protected intermediate followed by an additional purification step (preparative HPLC, basic conditions) resulted in **14** as a white solid (8 mg, 31%). ^{1}H NMR (400 MHz, CD_3OD) δ ppm 8.39 (d, *J* = 8.2 Hz, 2 H) 8.31 (d, *J* = 0.6 Hz, 1 H) 8.24 (dd, *J* = 8.5, 0.6 Hz, 1 H) 8.16 (d, *J* = 8.5 Hz, 1 H) 7.84−7.93 (m, 3 H) 7.74 (ddd, *J* = 8.5, 7.0, 1.3 Hz, 1 H) 5.85 (d, *J* = 2.5 Hz, 1 H) 3.66 (dt, *J* = 12.0, 2.7 Hz, 1 H) 3.41−3.50 (m, 1 H) 3.16 (td, *J* = 12.6, 3.3 Hz, 1 H) 1.77−1.89 (m, 2 H) 1.66−1.74 (m, 1 H) 1.26−1.41 (m, 3 H). LC-MS (ESI) *m/z*: 387 $[M + H]^+$.

*(erythro) (Piperidin-2-yl){2-[6-(trifluoromethyl)pyridin-3-yl]-quinolin-4-yl}methanol Dihydrochloride (**15**).* The compound was prepared according to the same procedure as **12** using 2-(trifluoromethyl)pyridine-5-boronic acid (11 mg, 0.057 mmol) as starting material and heating the reaction mixture for 5 h at 80 °C followed by 3 days at 65 °C. Deprotection of the Boc-protected intermediate resulted in **15** as a white solid (11 mg, 50%). ^{1}H NMR (400 MHz, CD_3OD) δ ppm 9.48 (s, 1 H) 8.82 (dd, 0 = 8.2, 1.9 Hz, 1 H) 8.42−8.52 (m, 2 H) 8.37 (d, *J* = 8.9 Hz, 1 H) 8.04−8.16 (m, 2 H) 7.94 (t, *J* = 7.4 Hz, 1 H) 6.03 (br. s., 1 H) 3.71 (d, *J* = 12.0 Hz, 1 H) 3.42−3.52 (m, 1 H) 3.18 (td, *J* = 12.9, 2.7 Hz, 1 H) 1.67−1.92 (m, 4 H) 1.31−1.44 (m, 2 H). LC-MS (ESI) *m/z*: 388 $[M + H]^+$.

*tert-Butyl (2S)-2-[(R)-(2-Bromoquinolin-4-yl) (hydroxy)methyl]-piperidine-1-carboxylate and tert-Butyl (2S)-2-[(S)-(2-Bromoquinolin-4-yl) (hydroxy)methyl]piperidine-1-carboxylate (**16**).* 2,4-Dibromoquinoline (450 mg, 1.60 mmol) was dissolved in dry THF (6 mL) under a nitrogen atmosphere. 1.3 M *i*-PrMgCl·LiCl in THF (1.50 mL, 1.90 mmol) was added slowly at 0 °C, and the reaction allowed to rise to rt over 30 min. *tert*-Butyl (2*S*)-2-formylpiperidine-1-carboxylate[34] (340 mg, 1.60 mmol) was dissolved in dry THF (50 mL) and added slowly to the reaction mixture, followed by stirring at rt for 4 h. Saturated NH_4Cl solution (50 mL) was added, and the mixture was extracted with ethyl acetate (3 × 20 mL). The combined organic layers were washed with brine (25 mL), dried over $MgSO_4$, filtered, and then evaporated in vacuo. The resulting colorless oil was purified by flash chromatography (ethyl acetate/heptane, 1:3). Fractions 10−17 were collected and dried under vacuum to give *tert*-butyl (2*S*)-2-[(*R*)-(2-bromoquinolin-4-yl) (hydroxy)methyl]piperidine-1-carboxylate (139 mg, 21%) as a white solid. LC-MS (API-ES) *m/z*: 421 $[M + H]^+$. Fractions 20−30 were collected and dried under vacuum to give *tert*-butyl (2*S*)-2-[(*S*)-(2-bromoquinolin-4-yl) (hydroxy)methyl]-piperidine-1-carboxylate (162 mg, 25%) as a white solid. LC-MS

DOI: 10.1021/acs.jmedchem.6b01009
J. Med. Chem. 2016, 59, 8577−8592

(API-ES) m/z: 421 $[M + H]^+$. The compounds were used in the next steps without further purification or characterization.

*tert-Butyl (2R)-2-[(S)-(2-Bromoquinolin-4-yl) (hydroxy)methyl]-piperidine-1-carboxylate and tert-Butyl (2R)-2-[(R)-(2-Bromoquinolin-4-yl) (hydroxy)methyl]piperidine-1-carboxylate (**17**).* The compound was prepared according to the same procedure as for **16** but using *tert*-butyl (2*R*)-2-formylpiperidine-1-carboxylate[34] as a starting material. Fractions 14−22 were collected and dried under vacuum to give *tert*-butyl (2*R*)-2-[(*S*)-(2-bromoquinolin-4-yl) (hydroxy)methyl]-piperidine-1-carboxylate (156 mg, 29%) as a white solid. LC-MS (API-ES) m/z: 421 $[M + H]^+$. Fractions 28−38 were collected and dried under vacuum to give *tert*-butyl (2*R*)-2-[(*R*)-(2-bromoquinolin-4-yl) (hydroxy)methyl]piperidine-1-carboxylate (150 mg, 28%) as a white solid. LC-MS (API-ES) m/z: 421 $[M + H]^+$. The compounds were used in the next steps without further purification or characterization.

*[(2S)-1-(Triphenylmethyl)piperidin-2-yl]methanol (**18**).* To an oven-dried three-neck flask (100 mL) equipped with a stir bar and a condenser was added THF (10 mL) under an atmosphere of nitrogen. To this, $LiAlH_4$ (0.47g, 12.6 mmol) was added, and the mixture was stirred to form a suspension. To this was added methyl (2*S*)-1-(triphenylmethyl)piperidine-2-carboxylate[32] (2.20 g, 8.42 mmol). The solution was allowed to stir for 3 h at rt. After 30 min 10 mL THF was added. The reaction mixture was then cautiously quenched with 1 M aqueous NaOH (1 mL) and H_2O (2 mL). Anhydrous $MgSO_4$ (approximately 1 g) was then added, and the solution was passed through a pad of Celite by the aid of 300 mL of DCM. The filtrate was then concentrated in vacuo. The residue was purified by flash chromatography (Et_3N/MeOH/DCM, 1:1:98) to give the title compound (1.71 g, 99%) as a white foam. $[\alpha]_D^{20}$ = +58.8 (*c* 0.5, DCM). ^{1}H NMR (400 MHz, DMSO-d_6) δ 7.42 (d, *J* = 7.6 Hz, 6H), 7.28 (t, *J* = 7.7 Hz, 6H), 7.15 (t, *J* = 7.7 Hz, 3H), 3.93−3.99 (m, 1H), 3.11−3.24 (m, 2H), 2.74−2.84 (m, 1H), 2.26−2.38 (m, 2H), 1.60−1.76 (m, 2H), 1.43−1.59 (m, 2H), 1.35 (br. s., 2H). ^{13}C NMR (101 MHz, DMSO-d_6) δ 144.9, 128.8, 127.7, 125.8, 77.2, 59.7, 56.1, 54.5, 42.1, 25.1, 18.6. LC-MS (API-ES) m/z: 116. $[M - Tr + H]^+$.

*(2S)-1-(Triphenylmethyl)piperidine-2-carbaldehyde (**19**).* To an oven-dried flask (100 mL) equipped with a stir bar (N_2) was added DCM (5.7 mL) and was then cooled to −78 °C. To this solution was slowly added oxalyl chloride (0.61 mL, 7.13 mmol), followed by dropwise addition of a solution of DMSO (0.84 mL, 11.9 mmol) in DCM (3.3 mL). The reaction was stirred for 10 min, and a solution of [(2*S*)-1-(triphenylmethyl)piperidin-2-yl]methanol (**18**) (1.7 g, 4.76 mmol) in DCM (4.28 mL) was added. The suspension was allowed to stir for 1.5 h, then TEA (2.65 mL, 19.0 mmol) was added, and the mixture was allowed to stir for an additional 1.5 h. The −78 °C bath was removed, 20 mL sat. NH_4Cl (aq)/28% NH_3 (2:1) was added, and the solution was partitioned between DCM (30 mL) and H_2O (30 mL). The layers were separated, and the aqueous layer was extracted with DCM (3 × 70 mL). The combined organic layers were dried over $MgSO_4$, filtered, and concentrated in vacuo. The residue was purified by flash chromatography (TEA/ethyl acetate/heptane, 1:9:90) to afford the title compound (1.54 g, 91%) as a white solid. $[\alpha]_D^{20}$ = +62.5 (*c* 0.5, DCM). ^{1}H NMR (400 MHz, DMSO-d_6) δ 8.43 (s, 1H), 7.42 (d, *J* = 7.4 Hz, 6H), 7.32 (t, *J* = 7.7 Hz, 6H), 7.16−7.24 (m, 3H), 3.55 (d, *J* = 1.7 Hz, 1H), 3.12−3.21 (m, 1H), 2.77 (s, 1H), 1.86−2.00 (m, 1H), 1.74−1.83 (m, 1H), 1.62−1.74 (m, 1H), 1.57 (d, *J* = 11.2 Hz, 2H), 1.01−1.18 (m, 1H). ^{13}C NMR (101 MHz, DMSO-d_6) δ 208.9, 143.4, 128.6, 128.2, 126.3, 76.9, 62.0, 43.1, 28.9, 25.2, 20.7. LC-MS (API-ES) m/z: 114 $[M - Tr + H]^+$.

*(R)-(2-Bromoquinolin-4-yl)[(2S)-1-(triphenylmethyl)piperidin-2-yl]methanol (**20**).* 2,4-Dibromoquinoline (1.61 g, 5.63 mmol) was dissolved in dry THF. 1.3 M *i*-PrMgCl·LiCl complex THF (6.6 mL, 8.66 mmol) was added dropwise at 0 °C. The reaction mixture was stirred at rt for 30 min. (2*S*)-1-(Triphenylmethyl)piperidine-2-carbaldehyde (**19**) (1.54 g, 4.33 mmol) dissolved in dry THF was added, and the reaction mixture was stirred at rt for 4 h. After the reaction was quenched with sat NH_4Cl (aq)/28% NH_3 (20 mL, 2:1) solution was added, and the mixture was extracted with DCM (3 × 20 mL). The organic phase was separated and washed with brine (25 mL). The solution was dried over $MgSO_4$, filtered, and then evaporated in vacuo. The resultant oil was purified by flash chromatography (TEA/ethyl acetate/heptane, 1:9:90). Fractions were collected and dried under vacuum to give title compound (1.19 g, 49%) as a white solid. $[\alpha]_D^{20}$ = insufficient material. ^{1}H NMR (400 MHz, DMSO-d_6) δ 7.92−7.98 (m, 1H), 7.81 (s, 1H), 7.70−7.76 (m, 1H), 7.38 (d, *J* = 7.0 Hz, 6H), 7.24 (s, 1H), 7.12−7.22 (m, 9H), 6.01 (d, *J* = 4.7 Hz, 1H), 5.72−5.80 (m, 1H), 3.68−3.76 (m, 1H), 3.60−3.68 (m, 1H), 2.95−3.05 (m, 1H), 1.65−1.83 (m, 1H), 1.20−1.31 (m, 1H), 0.95−1.13 (m, 4H), 0.07−0.28 (m, 1H). ^{13}C NMR (101 MHz, DMSO-d_6) δ 154.9, 148.1, 144.8, 141.6, 130.3, 129.8, 128.7, 127.6, 126.6, 126.0, 124.8, 124.7, 123.8, 78.4, 73.6, 55.6, 31.1, 22.6, 18.5, 14.0. LC-MS (API-ES) m/z: 321 $[M - Tr + H]^+$.

*(R)-[2-(4-Chlorophenyl)quinolin-4-yl][(2S)-1-(triphenylmethyl)-piperidin-2-yl]methanol (**21**).* Compound **20** (613 mg, 1.11 mmol) and 4-chlorophenylboronic acid (180 mg, 1.11 mmol) were dissolved in 2-MeTHF (5.5 mL) under N_2, and $PdCl_2$(dppf) (71 mg, 0.09 mmol) and 2 M aqueous K_2CO_3 (2.2 mL, 4.4 mmol) were added under nitrogen atmosphere. The reaction was heated at 90 °C overnight, filtrated, and dried under vacuum to give title compound as a white solid (650 mg, 99%). $[\alpha]_D^{20}$ = +8.5 (*c* 1.0, DCM). ^{1}H NMR (400 MHz, DMSO-d_6) δ 8.29−8.36 (m, 3H), 8.08 (dd, *J* = 1.0, 8.5 Hz, 1H), 7.71 (ddd, *J* = 1.1, 7.0, 8.4 Hz, 1H), 7.64−7.68 (m, 2H), 7.46 (br. d, *J* = 8.5 Hz, 1H), 7.30−7.38 (m, 6H), 7.21 (ddd, *J* = 1.3, 7.0, 8.4 Hz, 1H), 7.10 (d, *J* = 2.2 Hz, 8H), 5.94 (d, *J* = 4.7 Hz, 1H), 5.85 (t, *J* = 5.3 Hz, 1H), 3.71−3.82 (m, 2H), 2.95−3.05 (m, 1H), 1.73−1.88 (m, 1H), 1.20−1.30 (m, 2H), 1.08−1.15 (m, 1H), 0.97−1.07 (m, 2H), 0.08−0.25 (m, 1H). LC-MS (API-ES) m/z: 353 $[M - Tr + H]^+$.

*[(2R)-1-(Triphenylmethyl)piperidin-2-yl]methanol (**22**).* The compound was synthesized according to the same procedure as **18** but using (2*R*)-1-(triphenylmethyl)piperidine-2-carboxylate[32] (3.70 g, 9.62 mmol) as a starting material. The combined organic fractions were concentrated in vacuo to give the title compound (3.29 g, 98%) as a white foam. $[\alpha]_D^{20}$ = −64.1 (*c* 0.7, DCM). ^{1}H NMR (400 MHz, DMSO-d_6) δ 7.43 (d, *J* = 7.4 Hz, 6H), 7.28 (t, *J* = 7.7 Hz, 6H), 7.13−7.18 (m, 3H), 3.96 (t, *J* = 6.0 Hz, 1H), 3.18−3.25 (m, 1H), 3.17 (d, *J* = 3.8 Hz, 1H), 2.78 (br. s., 1H), 2.32 (br. s., 1H), 2.30 (s, 1H), 1.70 (br. s., 2H), 1.48 (br. s., 2H), 1.36 (d, *J* = 4.7 Hz, 2H). LC-MS (ESI^+) m/z 116 $[M - Tr + H]^+$.

*(2R)-1-(Triphenylmethyl)piperidine-2-carbaldehyde (**23**).* The compound was synthesized according to the same procedure as **19** but using **22** (31 g, 88 mmol) as a starting material. The residue was purified by flash chromatography (TEA/ethyl acetate/heptane, 1:9:90) to afford the title compound (22 g, 71%) as a white solid. $[\alpha]_D^{20}$ = −66.2 (*c* 0.8, DCM). ^{1}H NMR (400 MHz, DMSO-d_6) δ 7.42 (d, *J* = 7.6 Hz, 6H), 7.32 (t, *J* = 7.9 Hz, 6H), 7.16−7.23 (m, 3H), 3.52−3.59 (m, 1H), 3.11−3.21 (m, 1H), 2.73−2.83 (m, 1H), 1.86−2.00 (m, 1H), 1.74−1.83 (m, 1H), 1.62−1.74 (m, 1H), 1.50−1.62 (m, 2H), 1.02−1.18 (m, 1H). LC-MS (ESI^+) m/z 114 $[M - Tr + H]^+$.

*(S)-(2-Bromoquinolin-4-yl)[(2R)-1-(triphenylmethyl)piperidin-2-yl]methanol (**24**).* The compound was prepared according to the same procedure as for **20** but using **23** (7.8 g, 22 mmol) as starting material to give the title compound (11.4 g, 93%) as a white solid. $[\alpha]_D^{20}$ = insufficient material. ^{1}H NMR (400 MHz, DMSO-d_6) δ 7.95 (d, *J* = 8.4 Hz, 1H), 7.81 (s, 1H), 7.69−7.76 (m, 1H), 7.39 (d, *J* = 7.0 Hz, 6H), 7.24 (s, 2H), 7.10−7.21 (m, 9H), 6.00 (d, *J* = 4.7 Hz, 1H), 5.76 (t, *J* = 5.1 Hz, 1H), 3.59−3.76 (m, 2H), 2.92−3.05 (m, 1H), 1.67−1.83 (m, 1H), 0.96−1.13 (m, 4H), 0.10−0.29 (m, 1H). LC-MS (ESI^+) m/z 321, $[M - Tr + H]^+$.

*(S)-[2-(4-Chlorophenyl)quinolin-4-yl][(2R)-1-(triphenylmethyl)-piperidin-2-yl]methanol (**25**).* The compound was synthesized according to the same procedure as **21** but using **24** (8.52 g, 15.0 mmol) as starting material. The resulting solution was purified by passing through silica gel eluting with TEA/ethyl acetate/heptane (1:9:90). The filtrate was evaporated to give the title compound (7.8 g, 89%). $[\alpha]_D^{20}$ = −9.6 (*c* 0.6, DCM). ^{1}H NMR (400 MHz, DMSO-d_6) δ 8.27−8.35 (m, 3H), 8.08 (dd, *J* = 1.0, 8.5 Hz, 1H), 7.59−7.74 (m, 3H), 7.03−7.47 (m, 18H), 5.94 (d, *J* = 4.6 Hz, 1H), 5.82−5.90 (m, 1H), 3.69−3.86 (m, 2H), 2.92−3.09 (m, 1H), 1.72−1.92 (m, 1H), 1.23 (d, *J* = 0.8 Hz, 2H), 0.96−1.15 (m, 3H), 0.07−0.27 (m, 1H). LC-MS (ESI) m/z: 353, $[M - Tr + H]^+$.

DOI: 10.1021/acs.jmedchem.6b01009
J. Med. Chem. 2016, 59, 8577−8592

SXRD Experiments. Crystal data for *IIa*: $C_{45}H_{44}Cl_{11}N_4O_2$, M_r = 1062.79, monoclinic, space group *C*2 (no. 5), a = 29.758(2) Å, b = 5.9973(4) Å, c = 15.3874(10) Å, β = 118.372(3)°, V = 2416.3(3) Å^3, Z = 2, D_{calc} = 1.461 g × cm^{-3}, μ(MoKα) = 6.74 cm^{-1}, R = 0.041, wR^2 = 0.096, GOF = 0.88, Flack x = 0.02(8). The data were collected at 200 K on a Bruker APEXII diffractometer with graphite monochromated MoKα radiation (λ = 0.71073 Å) and employing a 0.09 × 0.11 mm × 0.31 mm crystal (3585 unique, R_{int} = 0.11). Crystal data for *IIb*: $C_{45}H_{44}Cl_{11}N_4O_2$, M_r = 1062.79, monoclinic, space group *C*2 (no. 5), a = 29.7509(14) Å, b = 5.9957(3) Å, c = 15.3980(8) Å, β = 118.340(3)°, V = 2417.5(2) Å^3, Z = 2, D_{calc} = 1.460 g × cm^{-3}, μ(Mo Kα) = 6.74 cm^{-1} R = 0.045, wR^2 = 0.11, GOF = 0.90, Flack x = 0.04(8). The data were collected at 200 K on a Bruker APEXII diffractometer with graphite monochromated MoKα radiation (λ = 0.71073 Å) and employing a 0.09 × 0.10 × 0.34 mm crystal (4423 unique, R_{int} = 0.106). CCDC-1427982 and CCDC-1427983 contains the supplementary crystallographic data for *IIa* and *IIb*. These data can be obtained free of charge from The Cambridge Crystallographic Data Centre (www.ccdc.cam.ac.uk/data_request/cif).

Cell Culture Conditions. GCs were grown in serum-free media supplemented with N2, B27, EGF, and FGF-2 (20 ng/mL) using previously described methodology (Pollard et al., 2009). Culture plates were precoated with Laminin (Sigma) for 3 h at 10 μg/mL prior to use, and 70% confluent cells were split 1:3 using TrypLE Express (Invitrogen). Cells were cultured at 37 °C and 5% CO_2.

In Vitro Viability Assay. To determine compound dose−response inhibition of glioma cell viability and determine induction of vacuolization, a 96-well PP (NUNC) compound plate was prepared by dispensing 15 μL of a 10 mM DMSO stock solution of the compound to be tested into column 1. Each row was serial diluted 2:1 into 100% DMSO, resulting in a serial dilution of each compound from 10 mM to 0.17 mM in columns 1−11 (10 μL/well). Negative (100% DMSO) and positive (**1** in 100% DMSO, 10 mM) controls were placed in rows 1−4 and 5−8, respectively, of column 12. The wells were diluted with 190 mL of the aforementioned cell culture media, and 5 μL of each well of compound solution transferred to quadruplicate wells of a sterile 384-well black clear bottom plate (BD Falcon) containing 2−3000 U3013 glioma cells at 70% confluency in 45 μL growth media. The plate was incubated for 48 h in the presence of compound, after which the plate was removed from the incubator, and five fields of each well imaged in bright-field using an Operetta High Content Imaging system (PerkinElmer) using a live cell chamber at 37 °C and 5% CO_2 to determine vacuole accumulation at each concentration. The plate was then allowed to cool to rt, and each well was treated with freshly prepared CellTiterGlo (Promega) reagent according to the manufacturer's instructions. The plate was shaken for 15 min, and luminescence measured using a Victor3 (PerkinElmer) microtiterplate reader. Total luminescence was normalized relative to negative control, and curve fitting performed using GraphPad Prism (v6.02) software.

Oral Bioavailability, in Vitro and in Vivo Pharmacokinetics. All animal experiments were performed at Adlego Biomedical, Stockholm, Sweden with authorization by the Stockholm Region's animal protection committee.

The pharmacokinetic properties of [*R*,*S*]**2** and [*S*,*R*]**2** were determined in male NMRI mice (Charles River, Germany) following single intravenous (i.v., tail vein, 2 mg/kg) or per oral (p.o, gavage, 20 mg/kg). Light isoflurane anesthesia was used at i.v. administration, and no anesthesia was used at p.o. administration. Blood samples were kept on ice after sampling and centrifuged at +4 °C, 1800 *g* for 5 min to prepare plasma. Blood and homogenized brain samples were taken from animals at the following nominal time points: 15, 30, and 60 min and 2, 4, 6, 8, 24, 48, 72, and 144 h after dosing (n = 3 samples/time-point). Blood sampling (400−600 μL) was performed by orbital plexus collection under isoflurane anesthesia into EDTA plasma tubes (BD Microtainer K2EDTA). Bioanalytical quantification of [*R*,*S*]**2** and [*S*,*R*]**2** was analyzed in plasma and brain samples by a UPLC-MS/MS. Pharmacokinetics were calculated by noncompartmental analysis (NCA) from composite (mean) profiles using Phoenix WinNonlin Professional (v 6.3). Nominal sampling times and dose levels have been used for the NCA calculations. All animals dosed with [*R*,*S*]**2** and [*S*,*R*]**2** were systemically exposed to the test compound. The plasma and brain concentrations were detectable and analyzed until 144 h. Brain sampling was performed after the end of blood sampling at the specified time points following euthanization and skull extraction. Brains were weighed, placed in test tubes, and placed on wet ice. 4 mL PBS (pH 7.4) per 1g of brain tissue was added to the test tube, and brains were then homogenized using an Ultra-Turrax T25 homogenizator (Setting 2, 9500 rpm, 10 s). The homogenates were frozen at −20 °C immediately after homogenization.

Protein binding was determined by Cyprotex Discovery Ltd., Macclesfield, U.K. Solutions of test compound (5 μM, 0.5% final DMSO concentration) were prepared in buffer (pH 7.4) and 100% mouse plasma. The experiment was performed using equilibrium dialysis with the two compartments separated by a semipermeable membrane. The buffer solution was added to one side of the membrane and the plasma solution to the other side. After equilibration, samples were taken from both sides of the membrane. Standards were prepared in plasma and buffer and incubated at 37 °C. Test compound incubations were performed in duplicate and expressed as averages. The solutions for each batch of compounds were combined into two groups (protein-free and protein-containing) and then cassette-analyzed by LC-MS/MS using two sets of calibration standards for protein-free (7 points) and protein-containing solutions (6 points). Samples were quantified using standard curves prepared in the equivalent matrix.

Zebrafish Xenograft Studies. All zebrafish experiments were conducted at Karolinska Institutet, following protocols that received institutional authorization by the Stockholm Region's animal protection committee.

Glioma Cell Labeling. U3013 glioblastoma cells (provided by U-CAN, Uppsala University) were cultured according to published protocol.[17] When the culture was approximately 70% confluent, live-cell labeling dye Cell Tracker (Life Technologies) was added directly to the medium at concentrations recommended by the manufacturer. The culture was incubated for 30 min and monitored under a fluorescent microscope to judge the extent of labeling.

Embryo Preparation. Zebrafish larvae were injected with Mitfa morpholino and allowed to grow in egg water until 2 days post-fertilization according to Kimmel.[37] Unfertilized eggs and larvae with developmental defects were manually removed. On 2 days post-fertilization, the larvae were anesthetized using 0.1% tricaine in egg water and mounted onto a Petri dish with agarose platform using a larval mold (Kit-79, Angthos). Upon mounting, fresh egg water with 0.1% tricaine was added to the Petri dish to keep the embryos submerged under water.

Cell Injection and Monitoring. The labeled cells were dissociated using Triple E medium (Gibco), as described by the manufacturer. Following dissociation, cells were pelleted using centrifugation at 1000 rpm for 5 min. The cell pellet was resuspended in 100 μL of PBS and put on ice. The cells were counted, and approximately 3000 cells were injected into the developing brain ventricle per embryo. Post-injection, partially or wrongly injected embryos were manually removed, and 0.1% tricaine egg water was replaced with fresh egg water. The injected embryos were allowed to recover for 30 min. Following recovery, the embryos were transferred into 96-well plates and taken for compound treatment.

Compound Treatment. Three embryos were transferred into each well of a clear polystyrene 96-well plate. Egg water (200 μL) containing DMSO or compound was added to each well. Fresh egg water (with or without compound) was replaced every 6 h for 10 days. After 10 days, the embryos were fixed and photographed.

■ ASSOCIATED CONTENT

Ⓢ Supporting Information

The Supporting Information is available free of charge on the ACS Publications website at DOI: 10.1021/acs.jmedchem.6b01009.

DOI: 10.1021/acs.jmedchem.6b01009
J. Med. Chem. 2016, 59, 8577−8592

Chromatograms from chiral separations, ^{1}H NMR spectra of [*R*,*S*]**2**, [*S*,*R*]**2**, [*R*,*R*]**3** and [*S*,*S*]**3**, purity, ee and yield of chiral HPLC separations. Analyses from stereoselective syntheses (PDF)
Compound data (CSV)

AUTHOR INFORMATION

Corresponding Author

*E-mail: lars.gj.hammarstrom@ki.se. Phone: +46 (0)733 745034.

Present Address

[∇]Leibniz-Institut für Molekulare Pharmakologie im Forschungsverbund Berlin e.V. (FMP), Campus Berlin-Buch, Robert-Roessle-Str. 10, 13125 Berlin, Germany

Notes

The authors declare the following competing financial interest(s): L.G.J.H., S.K., and P.E. are cofounders and hold interest in Glionova Therapeutics, which contributed to the funding of this work.

ACKNOWLEDGMENTS

This work was supported by VINNOVA, the Swedish Research Council, Knut and Alice Wallenbergs Foundation, Linné grants (DBRM grants), Swedish Cancer Foundation, Söderbergs Foundation, Glionova Therapeutics, and Karolinska Institutet. U3013 glioma cells were kindly provided by Lene Uhrbom and Karin Forsberg-Nilsson through U-CAN, Uppsala University. ChemAxon cheminformatics tools (Marvin, JChem for Excel, version 6.0.3) were used for IUPAC naming. ChemDraw (PerkinElmer, v 14.0.0.117) was used for rendering of chemical structures. The authors wish to thank Dongoh Kwak of Karolinska Institutet for imaging of cells and David Pekar and Lucia Kovac of OnTargetChemistry (Recipharm), Uppsala for analyses. The authors are indebted to Prof Peter Dinér of the Royal Institute of Technology (KTH) for kind assistance with polarimetry experiments.

ABBREVIATIONS USED

GBM, glioblastoma; WHO, World Health Organization; TMZ, Temozolomide; BBB, blood−brain barrier; VEGF, vascular endothelial growth factor; SXRD, single crystal X-ray diffraction; NMRI, Naval Medical Research Institute; PDA, photodiode array; TEA, trimethylamine; NCA, noncompartmental analysis

REFERENCES

(1) Omuro, A.; DeAngelis, L. M. Glioblastoma and Other Malignant Gliomas: A Clinical Review. *JAMA* **2013**, *310*, 1842−1850.

(2) Louis, D. N.; Ohgaki, H.; Wiestler, O. D.; Cavenee, W. K.; Burger, P. C.; Jouvet, A.; Scheithauer, B. W.; Kleihues, P. The 2007 WHO Classification of Tumours of the Central Nervous System. *Acta Neuropathol.* **2007**, *114*, 97−109.

(3) Stupp, R.; Mason, W. P.; van den Bent, M. J.; Weller, M.; Fisher, B.; Taphoorn, M. J. B.; Belanger, K.; Brandes, A. a; Marosi, C.; Bogdahn, U.; Curschmann, J.; Janzer, R. C.; Ludwin, S. K.; Gorlia, T.; Allgeier, A.; Lacombe, D.; Cairncross, J. G.; Eisenhauer, E.; Mirimanoff, R. O. Radiotherapy plus Concomitant and Adjuvant Temozolomide for Glioblastoma. *N. Engl. J. Med.* **2005**, *352*, 987−996.

(4) Weller, M.; Cloughesy, T.; Perry, J. R.; Wick, W. Standards of Care for Treatment of Recurrent Glioblastoma- Are We There Yet? *Neuro-Oncology* **2013**, *15*, 4−27.

(5) Johnson, B. E.; Mazor, T.; Hong, C.; Barnes, M.; Aihara, K.; McLean, C. Y.; Fouse, S. D.; Yamamoto, S.; Ueda, H.; Tatsuno, K.; Asthana, S.; Jalbert, L. E.; Nelson, S. J.; Bollen, A. W.; Gustafson, W. C.; Charron, E.; Weiss, W. A.; Smirnov, I. V.; Song, J. S.; Olshen, A. B.; Cha, S.; Zhao, Y.; Moore, R. A.; Mungall, A. J.; Jones, S. J. M.; Hirst, M.; Marra, M. A.; Saito, N.; Aburatani, H.; Mukasa, A.; Berger, M. S.; Chang, S. M.; Taylor, B. S.; Costello, J. F. Mutational Analysis Reveals the Origin and Therapy-Driven Evolution of Recurrent Glioma. *Science* **2014**, *343*, 189−193.

(6) Piccioni, D.; Lai, A.; Nghiemphu, P.; Cloughesy, T. Bevacizumab as First-Line Therapy for Glioblastoma. *Future Oncol.* **2012**, *8*, 929−938.

(7) Rinne, M. L.; Lee, E. Q.; Nayak, L.; Norden, A. D.; Beroukhim, R.; Wen, P. Y.; Reardon, D. a. Update on Bevacizumab and Other Angiogenesis Inhibitors for Brain Cancer. *Expert Opin. Emerging Drugs* **2013**, *18*, 137−153.

(8) Okonogi, N.; Shirai, K.; Oike, T.; Murata, K. Topics in Chemotherapy, Molecular-Targeted Therapy, and Immunotherapy for Newly-Diagnosed Glioblastoma Multiforme. *Anticancer Res.* **2015**, *1236*, 1229−1235.

(9) Hernández-Pedro, N. Y.; Rangel-López, E.; Vargas Félix, G.; Pineda, B.; Sotelo, J. An Update in the Use of Antibodies to Treat Glioblastoma Multiforme. *Autoimmune Dis.* **2013**, *2013*, 716813.

(10) Huang, R. Y.; Neagu, M. R.; Reardon, D. a.; Wen, P. Y. Pitfalls in the Neuroimaging of Glioblastoma in the Era of Antiangiogenic and Immuno/Targeted Therapy - Detecting Illusive Disease, Defining Response. *Front. Neurol.* **2015**, *6*, 1−16.

(11) Parrish, K.; Sarkaria, J.; Elmquist, W. Improving Drug Delivery to Primary and Metastatic Brain Tumors: Strategies to Overcome the Blood-Brain Barrier. *Clin. Pharmacol. Ther.* **2015**, *97*, 336−346.

(12) Carlsson, S. K.; Brothers, S. P.; Wahlestedt, C. Emerging Treatment Strategies for Glioblastoma Multiforme. *EMBO Mol. Med.* **2014**, *6*, 1359−1370.

(13) McLendon, R.; et al. Comprehensive Genomic Characterization Defines Human Glioblastoma Genes and Core Pathways. *Nature* **2008**, *455*, 1061−1068.

(14) Patel, A. P.; Tirosh, I.; Trombetta, J. J.; Shalek, A. K.; Gillespie, S. M.; Wakimoto, H.; Cahill, D. P.; Nahed, B. V.; Curry, W. T.; Martuza, R. L.; Louis, D. N.; Rozenblatt-Rosen, O.; Suvà, M. L.; Regev, A.; Bernstein, B. E. Single-Cell RNA-Seq Highlights Intratumoral Heterogeneity in Primary Glioblastoma. *Science* **2014**, *344*, 1396−1401.

(15) Reardon, D. a.; Wen, P. Y. Glioma in 2014: Unravelling Tumour Heterogeneity—implications for Therapy. *Nat. Rev. Clin. Oncol.* **2015**, *12*, 69−70.

(16) Ozawa, T.; Holland, E. C. Rethinking Glioma Treatment Strategy. *Oncotarget* **2014**, *5*, 9532−9533.

(17) Kitambi, S. S.; Toledo, E. M.; Usoskin, D.; Wee, S.; Harisankar, A.; Svensson, R.; Sigmundsson, K.; Kalderén, C.; Niklasson, M.; Kundu, S.; Aranda, S.; Westermark, B.; Uhrbom, L.; Andäng, M.; Damberg, P.; Nelander, S.; Arenas, E.; Artursson, P.; Walfridsson, J.; Forsberg Nilsson, K.; Hammarström, L. G. J.; Ernfors, P. Vulnerability of Glioblastoma Cells to Catastrophic Vacuolization and Death Induced by a Small Molecule. *Cell* **2014**, *157*, 313−328.

(18) Rapport, M.; Senear, A.; Mead, J.; Koepfli, J. The Synthesis of Potential Antimalarials. 2-Phenyl-Alpha-(2-Piperidyl)-4-Quinolinemethanols. *J. Am. Chem. Soc.* **1946**, *68*, 2697−2703.

(19) Brown, R. F.; Jacobs, T. L.; Winstein, M. C.; Levy, E. F.; Bryan, G. M.; Magnusson, A. B.; Miller, S. J.; Terek, J. A. Alpha-(2-Piperidyl)-2-Aryl-4-Quinolinemethanols. *J. Am. Chem. Soc.* **1946**, *68*, 2705−2708.

(20) Pinder, R. M.; Burger, A. Antimalarials. 11. (2-Piperidyl)- and -(2-Pyridyl)-2-Trifluoromethyl-4-Quinolinemethanols. *J. Med. Chem.* **1968**, *11*, 267−269.

(21) Trenholme, C. M.; Williams, R. L.; Desjardins, R. E.; Frischer, H.; Carson, P. E.; Rieckmann, K. H.; Canfield, C. J. Mefloquine (WR 142,490) in the Treatment of Human Malaria. *Science* **1975**, *190*, 792−794.

(22) Croft, A. M. A Lesson Learnt: The Rise and Fall of Lariam and Halfan. *J. R. Soc. Med.* **2007**, *100*, 170−174.

(23) Kaul, A.; Overmeyer, J. H.; Maltese, W. A. Activated Ras Induces Cytoplasmic Vacuolation and Non-Apoptotic Death in

DOI: 10.1021/acs.jmedchem.6b01009
J. Med. Chem. 2016, 59, 8577−8592

Glioblastoma Cells via Novel Effector Pathways. *Cell. Signalling* **2007**, *19*, 1034−1043.
(24) Overmeyer, J. H.; Kaul, A.; Johnson, E. E.; Maltese, W. a. Active Ras Triggers Death in Glioblastoma Cells through Hyperstimulation of Macropinocytosis. *Mol. Cancer Res.* **2008**, *6*, 965−977.
(25) Bhanot, H.; Young, A. M.; Overmeyer, J. H.; Maltese, W. a. Induction of Nonapoptotic Cell Death by Activated Ras Requires Inverse Regulation of Rac1 and Arf6. *Mol. Cancer Res.* **2010**, *8*, 1358−1374.
(26) Overmeyer, J. H.; Maltese, W. a. Death Pathways Triggered by Activated Ras in Cancer Cells. *Front. Biosci., Landmark Ed.* **2011**, *16*, 1693−1713.
(27) Maltese, W. a; Overmeyer, J. H. Methuosis: Nonapoptotic Cell Death Associated with Vacuolization of Macropinosome and Endosome Compartments. *Am. J. Pathol.* **2014**, *184*, 1630−1642.
(28) *Structure Informatics Tool (SIT) Software*; IS3 AB: Stockholm, Sweden, 2012; http://www.i3s-consulting.com/Software.html.
(29) Flack, H. D. On Enantiomorph-Polarity Estimation. *Acta Crystallogr., Sect. A: Found. Crystallogr.* **1983**, *39*, 876−881.
(30) Cahn, R. S.; Ingold, C.; Prelog, V. Specification of Molecular Chirality. *Angew. Chem., Int. Ed. Engl.* **1966**, *5*, 385−415.
(31) Duan, Z.; Li, X.; Huang, H.; Yuan, W.; Zheng, S.-L.; Liu, X.; Zhang, Z.; Choy, E.; Harmon, D.; Mankin, H.; Hornicek, F. Synthesis and Evaluation of (2-(4-Methoxyphenyl)-4-quinolinyl)(2-Piperidinyl)-methanol (NSC23925) Isomers to Reverse Multidrug Resistance in Cancer. *J. Med. Chem.* **2012**, *55*, 3113−3121.
(32) León, B.; Fong, J. J. C. N.; Peach, K. K. C.; Wong, W. R.; Yildiz, F. H.; Linington, R. G. Development of Quinoline-Based Disruptors of Biofilm Formation Against Vibrio Cholerae. *Org. Lett.* **2013**, *15*, 1234−1237.
(33) Xie, Y.; Bergström, T.; Jiang, Y.; Johansson, P.; Marinescu, V. D.; Lindberg, N.; Segerman, A.; Wicher, G.; Niklasson, M.; Baskaran, S.; Sreedharan, S.; Everlien, I.; Kastemar, M.; Hermansson, A.; Elfineh, L.; Libard, S.; Holland, E. C.; Hesselager, G.; Alafuzoff, I.; Westermark, B.; Nelander, S.; Forsberg-Nilsson, K.; Uhrbom, L. The Human Glioblastoma Cell Culture Resource: Validated Cell Models Representing All Molecular Subtypes. *EBioMedicine* **2015**, *2*, 1351−1363.
(34) Balboni, G.; Marastoni, M.; Merighi, S.; Andrea Borea, P.; Tomatis, R. Synthesis and Activity of 3-Pyridylamine Ligands at Central Nicotinic Receptors. *Eur. J. Med. Chem.* **2000**, *35*, 979−988.
(35) Kegelman, T. P.; Hu, B.; Emdad, L.; Das, S. K.; Sarkar, D.; Fisher, P. B. In Vivo Modeling of Malignant Glioma: The Road to Effective Therapy. In *Advances in Cancer Research*; Tew, K. D., Fisher, P. B., Eds.; Elsevier Inc.: San Diego, 2014; Vol. *121*, pp 261−330.
(36) Yang, X.-j.; Cui, W.; Gu, A.; Xu, C.; Yu, S.-c.; Li, T.-t.; Cui, Y.-h.; Zhang, X.; Bian, X. wu. A Novel Zebrafish Xenotransplantation Model for Study of Glioma Stem Cell Invasion. *PLoS One* **2013**, *8*, e61801.
(37) Kimmel, C. B.; Ballard, W. W.; Kimmel, S. R.; Ullmann, B.; Schilling, T. F. Stages of Embryonic Development of the Zebrafish. *Dev. Dyn.* **1995**, *203*, 253−310.

DOI: 10.1021/acs.jmedchem.6b01009
J. Med. Chem. 2016, 59, 8577−8592